

2016-12-23

# The Use of M-Sequences to Optimize Underwater Acoustic Communications in Shallow Waters

Fabio B. Louza

*University of Miami*, [fabiolouza@hotmail.com](mailto:fabiolouza@hotmail.com)

Follow this and additional works at: [https://scholarlyrepository.miami.edu/oa\\_theses](https://scholarlyrepository.miami.edu/oa_theses)

---

## Recommended Citation

Louza, Fabio B., "The Use of M-Sequences to Optimize Underwater Acoustic Communications in Shallow Waters" (2016). *Open Access Theses*. 648.

[https://scholarlyrepository.miami.edu/oa\\_theses/648](https://scholarlyrepository.miami.edu/oa_theses/648)

This Open access is brought to you for free and open access by the Electronic Theses and Dissertations at Scholarly Repository. It has been accepted for inclusion in Open Access Theses by an authorized administrator of Scholarly Repository. For more information, please contact [repository.library@miami.edu](mailto:repository.library@miami.edu).

UNIVERSITY OF MIAMI

THE USE OF M-SEQUENCES TO OPTIMIZE UNDERWATER ACOUSTIC  
COMMUNICATIONS IN SHALLOW WATERS

By

Fabio B. Louza

A THESIS

Submitted to the Faculty  
of the University of Miami  
in partial fulfillment of the requirements for  
the degree of Master of Science

Coral Gables, Florida

December 2016

©2016  
Fabio B. Louza  
All Rights Reserved

UNIVERSITY OF MIAMI

A thesis submitted in partial fulfillment of  
the requirements for the degree of  
Master of Science

THE USE OF M-SEQUENCES TO OPTIMIZE UNDERWATER ACOUSTIC  
COMMUNICATIONS IN SHALLOW WATERS

Fabio B. Louza

Approved:

\_\_\_\_\_  
Harry A. DeFerrari, Ph.D.  
Professor of Applied Marine Physics

\_\_\_\_\_  
Arthur J. Mariano, Ph.D.  
Professor of Meteorology &  
Physical Oceanography

\_\_\_\_\_  
Michael G. Brown, Ph.D.  
Professor of Applied Marine Physics

\_\_\_\_\_  
Guillermo Prado, Ph.D.  
Dean of the Graduate School

LOUZA, FABIO B.

(M.S., Applied Marine Physics)  
(December 2016)

The Use of M-Sequences to Optimize  
Underwater Acoustic Communications  
in Shallow Waters

Abstract of a thesis at the University of Miami.

Thesis supervised by Professor Harry A. DeFerrari.

No. of pages in text. (68)

The relationship between dynamic ocean acoustic fluctuations and the underwater communication in shallow waters acoustic propagation channels will be investigated, as they present a challenging environment for the transmission of information, causing inter-symbol interference (ISI) and multipath signal spreading and fading. The study and simulations will be based on data from an upwelling monitoring buoy located in the shallow waters of Arraial do Cabo – Brazil. The focus of this thesis is to perform a systematic analysis of the role of the internal waves and upwelling on phase stability of a signal propagating through the channel, in terms of temporal coherence, using the Monterey-Miami parabolic equation (MMPE) model, and compare two approaches to optimize communication systems: prediction and/or measurement of the channel pulse responses. The first one is based on previous predicted pulse responses, given by MMPE and a matched or inverse filter to retrieve the message through multipath recombination. However, as filtering results begin to erode with time, one can estimate the refresh time of the filters necessary to keep up with real time varying sound speed profiles in these shallow waters. The second approach uses a simultaneous background experiment to directly measure and update the channel pulse response while collecting the message,

based on “training pulse response measurements”, classic low intensity M-sequences. Finally, the process called Hyperslice Cancellation by Coordinate Zeroing (HCCO) (Chang, 1992) will be performed to eliminate interferences between the M-sequences and the original messages.

## **Dedication**

To my parents Nilton and Angela, to my brothers Marcelo and Isabel, to my grand-aunt Arminda and to my beloved wife Cristiane and son Pedro Henrique for their unconditional love and support.

## **Acknowledgements**

This work has been a long journey involving several special persons to whom I must forward my appreciation. First of all, thanks God for your blesses and support during those moments of uncertainty and fear. Our private conversations calmed down my heart and guided me to the light. To Saint Jude Thaddeos, thanks for your silent support during my innumerous prays.

I would like to appreciate my advisor Dr. Harry DeFerrari for his encouragement and support during this amazing adventure through the Underwater Acoustics field. During these two years, Harry was always available to my questions and doubts, showing me the correct path to find a solution to the innumerous problems that appeared in this work. His passion for teaching is something really rare to find nowadays. Thanks Professor for being not only my advisor but a friend during this time in Miami, despite your busy life in the university. I also appreciate my committee members and some professors. Many thanks to Dr. Michael Brown, for introducing me to the fantastic field of Acoustics. To Dr. Jorge Willemsem and Dr. Arthur Mariano, thanks for your support and valuable advices to improve my thesis. I am very glad and honored in having you as professors at RSMAS.

Furthermore, I would like to thank my friend Fernando Monteiro for his friendship and moral support during my stay in Miami. One of the best Brazilian Navy Officers, and a Ph.D. candidate at RSMAS, Fernando always gave me smart suggestions during this time. To Brazilian friends and RSMAS colleagues, thank you for your cooperation and friendship. Many thanks also to my classmate Lisa Nyman for her encouragement and support. I wish her success and all the best in her Ph.D. and future career.



I would like to appreciate the sponsorship provided by the Brazilian Navy (Institute of Sea Studies Admiral Paulo Moreira), and to thank Captain Marcus Simões, my friends Lt Cmd Felipe Messias, a former RSMAS student and Mr. Fabio Contrera for their support and feedback during my studies.

Finally, I must appreciate my family members. Thanks Dad and Mom, Nilton and Angela, for your love and guidance since I was a child. Your faith that only education could lead me to the success was right. I will always love you. To my brothers Marcelo and Isabel, I thank for their love and encouragement. To my grand-aunt Arminda , a former elementary teacher, who always supported and incentivized me to join the Navy and reach my goals through education, but who passed away during this adventure, my most deep appreciation. To my mother-in-law Neusa, thanks for your love and support.

At last but most important, I thank my wife Cristiane and son Pedro Henrique for their patience, courage and love. This stay in Miami was a great challenge for all of us. But we proved that we are stronger together, going back to Brazil full of wonderful memories in our minds and friends in our hearts. Thank you so much for everything. Your unconditional love, support and encouragement were fundamental for the success of this work. I will love you forever!!!

## TABLE OF CONTENTS

	Page
LIST OF FIGURES.....	vii
LIST OF TABLES.....	x
LIST OF ACRONYMS/ABBREVIATIONS.....	xi
LIST OF SYMBOLS.....	xii
 Chapter	
1 INTRODUCTION .....	1
1.1 Motivation.....	2
1.2 Objectives.....	4
1.3 Background Theory.....	5
2 METHODOLOGY .....	13
2.1 Modeling Parameters .....	13
2.2 Digital Communications Systems.....	18
2.3 Method to improve UW Digital Communications.....	25
3 TEMPORAL COHERENCE AND THE IF REFRESH TIME.....	29
3.1 Analysis of the Temporal Coherence and Inverse Filter .....	33
3.2 Discussion.....	49
4 METHOD TO IMPROVE UW DIGITAL COMMUNICATIONS USING M-SEQUENCES.....	50
4.1 Describing the method .....	51
4.2 Simulation Parameters .....	52
4.3 Results.....	53
4.4 The influence of the noise level and amplitude relation over BER .....	59
4.5 Discussion.....	62
5 CONCLUSIONS AND FUTURE WORK.....	64
 References.....	 67

## LIST OF FIGURES

Figure 1.1- Extract of the Brazilian Nautical Chart 1508.....	3
Figure 1.2- Wind direction and SST.....	4
Figure 1.3- Multipath in the underwater channel.....	7
Figure 1.4- Inter-symbol Interference between 3 sequential bits.....	8
Figure 1.5- Channel PR measurement using M-sequences.....	12
Figure 2.1- Vertical Temperature Profiles.....	15
Figure 2.2- Sound Speed Profiles – Upwelling event .....	15
Figure 2.3- Evolution of Sound Speed Profiles in time.....	16
Figure 2.4- Sound Speed Profiles CTD (200m deep channel).....	17
Figure 2.5- Digital Communications System.....	18
Figure 2.6- Example of a positive and negative bit.....	19
Figure 2.7- Example of Channel PR.....	19
Figure 2.8- Simulation of 1 Bit propagating through the channel.....	21
Figure 2.9- Channel Pulse Response in noise.....	22
Figure 2.10- Transmission and Inverse filtering of 2 bits.....	24
Figure 2.11- Bit stream componentes.....	26
Figure 2.12- Energy pulse compression by FHT.....	27
Figure 2.13- Message in noise after FHT.....	28
Figure 3.1- Temperature profiles and Wind direction.....	30
Figure 3.2- Sound Speed Profiles for different ocean temperature conditions.....	31
Figure 3.3- Received pulse and predicted PR – Iso Warm SSP - 800Hz.....	34
Figure 3.4- Received pulse and predicted PR – Iso Cold SSP - 800Hz.....	35

Figure 3.5- Temporal Coherence and Inverse Filter – Iso Warm SSP - 800Hz.....	36
Figure 3.6- Temporal Coherence and Inverse Filter – Iso Cold SSP - 800Hz.....	36
Figure 3.7- Received pulse and predicted PR – Iso Warm SSP - 3200Hz.....	37
Figure 3.8- Received pulse and predicted PR – Iso Cold SSP - 3200Hz.....	38
Figure 3.9- Temporal Coherence and Inverse Filter – Iso Warm SSP - 3200Hz.....	39
Figure 3.10- Temporal Coherence and Inverse Filter – Iso Cold SSP - 3200Hz.....	39
Figure 3.11- Received pulse and predicted PR – Upwelling SSP - 800Hz.....	41
Figure 3.12- Received pulse and predicted PR - Upwelling SSP 3200Hz .....	41
Figure 3.13- Temporal Coherence and Inverse Filter 800Hz - Upwelling SSP.....	42
Figure 3.14- Temporal Coherence and Inverse Filter 3200Hz - Upwelling SSP.....	43
Figure 3.15- Vertical Temperature Profiles and IW Tidal energy.....	45
Figure 3.16- Received pulse and predicted PR – IW SSP - 800Hz.....	47
Figure 3.17- Received pulse and predicted PR – IW SSP - 3200Hz.....	47
Figure 3.18- Temporal Coherence and Inverse Filter 800Hz - IW SSP.....	48
Figure 3.19- Temporal Coherence and Inverse Filter 3200Hz - IW SSP.....	48
Figure 4.1- Bit streams composed of M-Seq + Message.....	52
Figure 4.2- Predicted PR and received Bit Stream in noise – 50m/3200Hz.....	54
Figure 4.3- Pulse compressed by FHT, Measured PR and Message – Depth:50m.....	55
Figure 4.4- Transmitted/Retrieved message after matched filter - 50m/3200Hz.....	56
Figure 4.5- Predicted PR and received Bit Stream in noise – 200m/3200Hz .....	57
Figure 4.6- Pulse compressed by FHT, Measured PR and Message– Depth:200m .....	58
Figure 4.7- Transmitted/Retrieved message after matched filter - 200m/3200Hz .....	58
Figure 4.8- Estimation of BER for several SNR for a 50m deep channel .....	61

Figure 4.9- Estimation of BER for several SNR for a 200m deep channel ..... 62

## LIST OF TABLES

Table 4.1- Amplitude 10/1, SNR and BER for 50m and 200m deep channel ..... 60

Table 4.2- Amplitude 10/5, SNR and BER for 50m and 200m deep channel ..... 60

## LIST OF ACRONYMS/ABBREVIATIONS

AWGN	Additive White Gaussian Noise
BER	Bit Error Rate
FHT	Fast Hadamard Transform
HCC0	Hyperslice Cancellation by Coordinate Zeroing
IEAPM	Brazilian Navy Institute of Sea Studies “Admiral Paulo Moreira”
IF	Inverse Filter
IFHT	Inverse Fast Hadamard Transform
ISI	Inter-symbol Interference
IW	Internal Waves
MF	Matched filter
MMPE	Monterey-Miami Parabolic Equation
PR	Channel pulse Response
SACW	South Atlantic Central Water
SISO	Single source and receiver / Single input and output
SNR	Signal to Noise Ratio
SRBR	Surface-reflected-bottom-refracted
SSP	Sound Speed Profile
SW	Shallow Water
UAC	Underwater Acoustic Channel
UW	Under Water
VTP	Vertical Temperature Profile

## LIST OF SYMBOLS

$\Delta T$  Experimental time

$^{\circ}C$  Celsius

COH Coherence

$C(z)$  Depth dependent SSP

dB Decibel

$f_c$  Carrier frequency

fft Fast Fourier Transform

$f(t)$  Function  $f$  in the time domain

Hz Hertz

ifft Inverse Fast Fourier Transform

Km Kilometer

m Meter

min Minutes

m/s Meters/Second

$p(t)$  Pulse response

s Seconds

$S_d$  Source depth

SPL Sound Pressure Level

$R_d$  Receiver depth

$t$  Arrival time

$T$  Coherence lag time



## **CHAPTER 1**

### **INTRODUCTION**

The basic layout of any underwater acoustic communication system contains a transmitter to send modulated information, the channel through which sound waves propagate and a receiver to recover the original information through some equalization process. However, the underwater environment is recognized as one of the most difficult communication medium in use today (Stojanovic and Preisig, 2009). Due to several physical phenomena that affect and delay the propagation, leading to significant distortions of the signal transmitted through this time and space varying channel, the underwater acoustic channel has grown in interest, in the last decades, due to its numerous civilian and military applications, such as transmitting data and information between ships and/or submarines or just monitoring the underwater environment.

Research on sound transmission has been underway for decades with the objective to understand how variability of the ocean environment causes fluctuations of the acoustic channel, limiting the reliability of the communication (DeFerrari, 2009). Furthermore, the intensity of the signal and its coherence at receiver are both important for underwater communication purposes (Song et al., 2012).

The acoustic coherence of a signal in the ocean implies its phase stability in time and/or space, being fundamental to permit signal processing techniques to achieve some gain over the background noise. However, coherence stability is directly affected by the fluctuations in the sound speed profiles which are time, depth and range dependent and by multipath propagation due to successive reflections at boundaries, surface and bottom, and refractions due to sound speed depth dependency. An acoustic signal propagates

through the channel along distinct paths of particular durations and trajectories and as the propagation speed of sound in the ocean is much lower compared to an electromagnetic wave, both the main signal and many delayed echoes arrive at receiver at different travel times, causing fading and severe inter-symbol interference, degrading the digital communications system performance (Lurton, 2002). Moreover, attenuation of the signal increases with frequency, limiting the bandwidth and so the data rate and the presence of ambient noise due to both natural and man-made sources also affect the filtering process to retrieve transmitted signals at the receiver.

In any communication media, if the channel impulse response is known, the transmitted signal can be decoded at receiver correctly at any time, even for a fast time varying ocean which is coherent and stable for only a few minutes in general. Thus, much effort has been done to correctly model and estimate the underwater channel pulse responses to establish a reliable acoustic communication link.

This way, this work will focus on important concepts such as Temporal Coherence, Inverse and Matched filters and present a method to estimate the channel pulse response and send messages simultaneously using M-sequences and Hadamard transforms.

## **1.1 MOTIVATION**

The Brazilian Navy Institute of Sea Studies “Admiral Paulo Moreira” (IEAPM), sponsor of this work, is located at Arraial do Cabo (23°S/042°W), near to Cabo Frio (Cold Cape), a coastal city of Rio de Janeiro state, where intense upwelling processes occur. Thus, the IEAPM performs and develops several projects related to underwater

acoustics in these shallow waters, a challenging environment to establish reliable underwater communications.

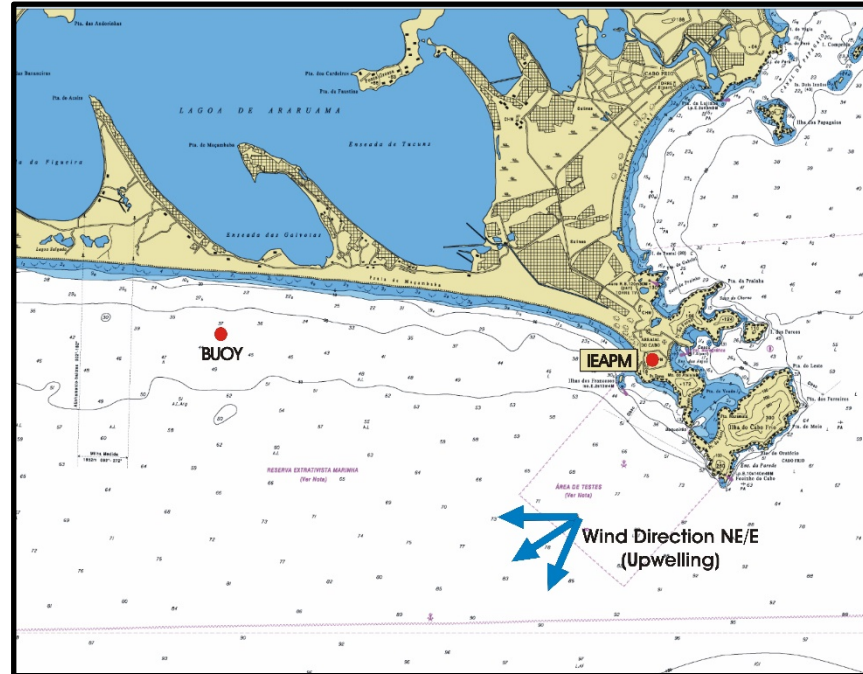


Figure 1.1: Extract of the Brazilian Nautical Chart 1508

### The upwelling phenomena

The coastal upwelling phenomena at Cabo Frio is defined as the ascending motion of cold and deep waters to the surface of the ocean due to the action of the predominant Northeast/East wind blowing regime. Typically parallel to the coast, the NE/E winds exist during the whole year, pushing huge amounts of surface waters to the sea as a consequence of the Ekman transport which states that the integrated flow of the near-surface ocean flows at  $90^\circ$  angle to the left of the wind in the Southern hemisphere. To keep the ocean in balance, cold and nutrient-rich waters ascend to the surface and the upwelling event is significant when the sea surface temperature reaches  $18^\circ\text{C}$  (Figure

1.2), the same of the deep South Atlantic Central Water (SACW), being more intense on summer due to the shallowness of the thermocline in this season (Torres, 1995). However, the upwelling process is interrupted by the passage of Frontal systems which turns wind direction to SW/W, causing a downwelling in the region.

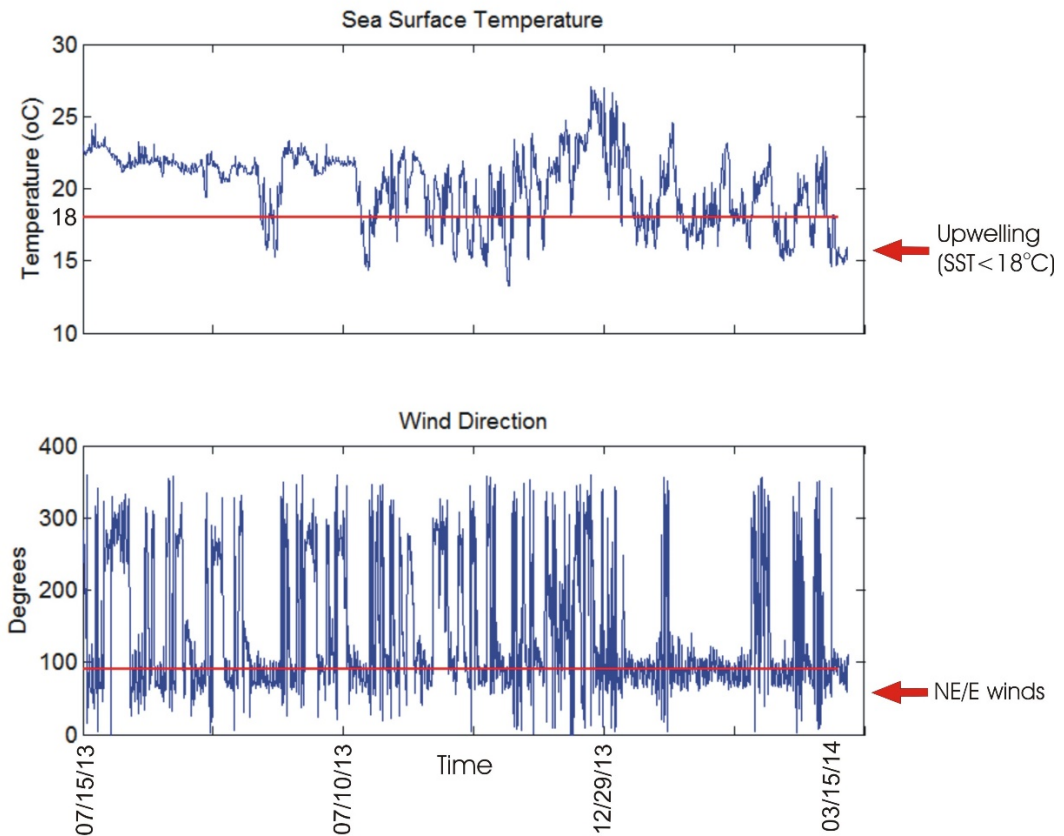


Figure 1.2: Wind direction and SST

## 1.2 OBJECTIVES

The first goal of this thesis is to perform a systematic analysis of the role of the upwelling events on phase stability of a signal propagating through a flat channel, for a fixed single source and receiver (SISO) scheme, based on predicted pulse responses given by MMPE model for several configurations of input parameters and an inverse

filter to retrieve the signal through multipath recombination in a no noise environment, estimating the refresh time of the filters necessary to keep up with real time varying sound speed profiles in these shallow waters.

The second goal is to introduce a method to optimize the underwater communications in shallow waters which directly measure and update the channel pulse response while collecting the message, simultaneously. The method is based on a transmission of a classic low intensity pseudo-random maximum length sequences (M-sequences) added to a phase shifted binary message in the presence of a background noise. To eliminate interferences between the M-Sequences and the transmitted message, a process called Hyperslice Cancellation by Coordinate Zeroing (HCC0) (Chang, 1992) based on pulse compression using Hadamard transforms and a matched filter will be performed. The results will be expressed and compared in terms of Bit Error Rate, an estimate of bit error probability used in binary communications.

### **1.3 BACKGROUND THEORY**

#### **Monterey-Miami Parabolic Equations model (MMPE)**

There are several models to compute solutions of the wave equation, but just a few are both depth and range dependent (Jensen et al, 2011). The parabolic-equation methods, introduced into underwater acoustics by Hardin and Tappert in the 70's, provide numerical solutions to the Helmholtz equation based on Fast Fourier Transforms. The Monterey-Miami Parabolic Equation (MMPE) model is a broadband, full-wave acoustic propagation model and has been widely used by researchers in this field, to model the acoustic channel, especially in shallow waters due to its fast implementation and

computational efficiency (Smith, 2000). The MMPE model utilizes the split-step Fourier marching algorithm based on the parabolic approximation to the Helmholtz equation, computing both the ocean impulse responses and frequency responses for several receiver depths and ranges, based on some input parameters such as the source frequency and depth, frequency bandwidth, sound speed profiles, channel depth and bathymetry.

Furthermore, the MMPE provides the Transmission Loss of the channel, defined as the ratio in decibels between the acoustic intensity at a field point and the intensity at 1-m distant from the source, and considered as the sum of a loss due to geometrical spreading, signal weakening as it propagates outward from source, and loss due to attenuation (Jensen et al, 2011).

However, in this work, the most important and useful results from MMPE will be the channel pulse responses in time domain. Each transmission will be simulated for some center frequency  $f_c$  and bandwidth of 25% of  $f_c$ , allowing the identification of multipath by arrival time. These results will permit the estimation of the temporal coherence for different frequency signals and the understanding of how each input parameter affect the propagation through the channel.

### **Multipath and Inter-symbol Interference**

In this work, “shallow water” means a water depth in which sound is propagated to the far-field a distance by repeated reflections from surface and bottom (Urick, 1983). Furthermore, the sound speed profiles which are time, depth and range dependent also affect the acoustic propagation. In underwater acoustics, due to the low sound speed compared to the speed of light, the main direct pulse arrives along with several time delayed pulses created by multiple reflections at boundaries causing fading and severe

inter-symbol interference creating distinguishable echoes and reverberation effects (Lurton, 2002).

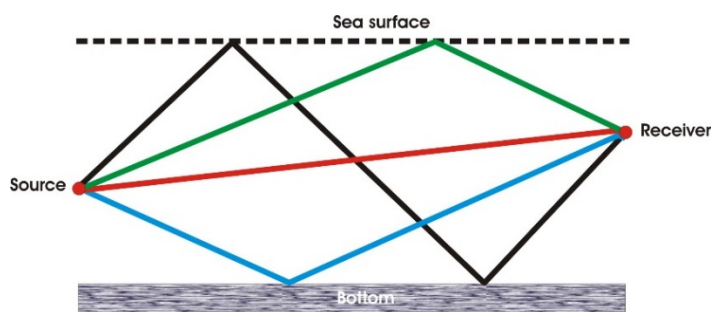


Figure 1.3: Multipath in the underwater channel

Above, figure 1.3 shows some possible multipath in the underwater channel. The direct path, surface reflected, bottom reflected and surface/bottom reflected are shown in red, green, blue and black, respectively.

Due to these multipath, the main arrival can be recorded at receiver with its own echoes as well as some very delayed echoes from the symbol transmitted before, causing inter-symbol interference. Thus, each symbol of the binary sequence spread to the adjacent symbol, degrading the system performance (Jeruchim et al, 2002). In the figure 1.4, one can understand how the ISI occur based on a simulated transmission of only 3 bits at 3200Hz. Close to the source, there is almost no ISI. However, 10Km far from the source, severe ISI occur due to the multipath.

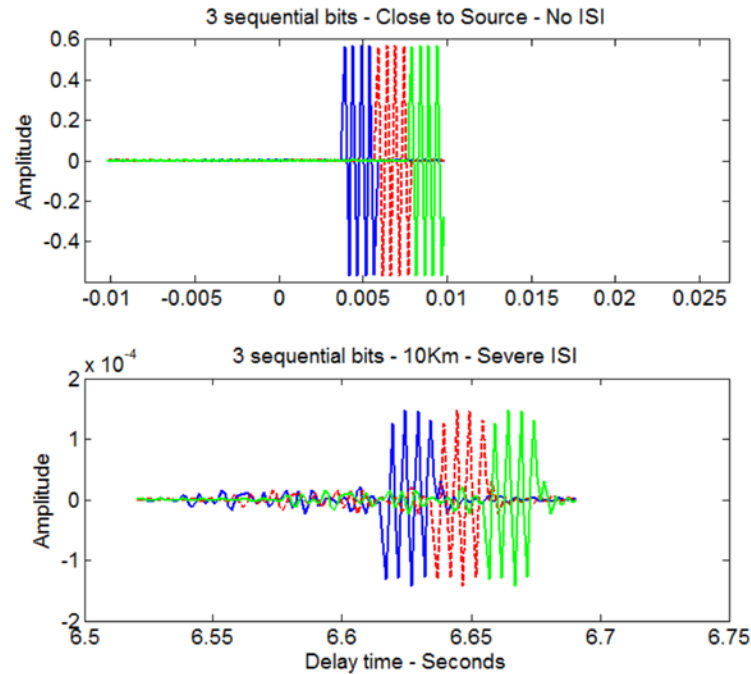


Figure 1.4: Inter-symbol Interference between 3 sequential bits

### Temporal Coherence

The temporal coherence is a statistical measure of the change of a wave form in time, being a complex quantity that depends on both amplitude and phase (DeFerrari, 2008). In the fast time varying ocean, the coherence phase stability of a signal propagating through the underwater channel is directly affected by the fluctuations in the sound speed profiles which are time, depth and range dependent and by multipath propagation due to successive interactions with boundaries.

Based on channel pulse responses versus arrival time, estimated by MMPE model, the temporal coherence of individual arrivals can be calculated as a time lagged covariance over the time history of the pulse responses  $p(t)$  as follows, where  $\Delta T$  is the experimental time, the time window of the simulations and  $T$  is the coherence lag time, generally 1 minute between consecutives PR:



$$coh(t, \tau) = \frac{\langle p(t, T)p(t, T + \tau) \rangle_{\Delta T}^2}{\langle p(t, T)^2 \rangle_{\Delta T} \langle p(t, T + \tau)^2 \rangle_{\Delta T}}.$$

Thus, basically, one impulse response  $p(t)$  is taken as a reference and cross correlated to several later pulses  $p(t+\tau)$  to obtain the temporal coherence curve at different times, letting one to estimate how long the channel remains coherent enough to permit communications.

### **Maximum Length Sequences (M-Sequences)**

Maximum Length Sequences (M-Sequences) have been used extensively in underwater acoustics experiments to derive channel impulse responses with accuracy between the source and receiver and are directly related to Hadamard transforms and cross-correlation technique (Chang, 1992). They are defined as a periodic pseudo random binary sequences, generated by a shift register with feedback with length or period  $P=2^N-1$ , where  $N$  is an integer. To convert the generated sequence in terms of 0 and 1's to a signal, it is mapped and represented only by +1 and -1's.

One of the most important property of the M-sequences is their perfect autocorrelation, represented by a Dirac delta function, presenting no time leakages. They are considered the “Gold Standard” of travel time measurements, being used for temporal coherence experiment for years (DeFerrari, 2008). Moreover, they share some statistical properties with white noise such as flat power spectrum density over a wide frequency range. But as the sequence is deterministic, generated by the shift registers, it is called pseudo-noise or pseudo-random sequence, avoiding interception of the transmitted signals.

## The Hadamard Transforms

The Fast Hadamard Transforms provide an efficient numerical method to cross-correlate M-sequences using only additions and subtractions and to estimate the channel pulse response. The cross correlation below is executed using matrix operations:

$$\underline{h} = \underline{P}_2 H(\underline{P}_1 \underline{s}), \text{ where:}$$

$\underline{h}$  : channel pulse response;

$\underline{s}$  : samples of the measured sequence;

$P_1/P_2$ : permutation vectors;

H: Hadamard matrix;

The Hadamard matrix is of a Sylvester type, square of dimension  $N=2^n$ , expressed by mutually orthogonal rows in terms of +1 or -1. Further, it can be constructed recursively as follows:

$$H_1 = 1, \quad H_2 = \begin{pmatrix} H_n & H_n \\ H_n & -H_n \end{pmatrix}$$

The Hadamard matrix is directly related to maximum length sequences. The reason is that one can generate a Hadamard matrix arranging M-Sequences in rows, shifted by one column and performing some column permutations.

As the M Sequence length/period (P) becomes large, the correlation detection becomes computationally intensive, on the order of  $P^2$  operations where  $P=2^N-1$ . But due to the similarity between M-sequences and Hadamard matrices, the FHT can do the pulse compression correlation much faster. Mapping the rows of the vector s in an appropriate way and using a butterfly algorithm, the number of operations to

crosscorrelate the received signal to the original M-Sequence can be reduced to  $P \cdot \log_2 P$ , instead of  $P^2$ , drastically reducing the computational time.

Furthermore, an important property of FHT is that it does not change the energy of the signal after pulse compression. Thus one can improve the signal to noise ratio (SNR) in  $10 \cdot \log_{10}(P)$  decibels (dB) as FHT only compress the M-Sequence energy in the first part of the channel pulse response, being the energy of noise spread over the remaining sequence length (Bjor, 2000).

### **Measurement of the Channel Pulse Response using M-Sequences**

Birdsaw (1966) and Metzger (1983) have been using M-sequences in underwater acoustics experiments for a long time, developing numerical methods to obtain high processing gain after pulse compression. DeFerrari and Rogers (2009) used important concepts for this thesis in their work, transmitting M-sequences, pulse compressing them using Fast Hadamard Transforms and coordinate zeroing (HCC0) to estimate the channel pulse responses for a bi-static active sonar.

$$y(t) = \int_{-\infty}^{\infty} x(\tau)h(t-\tau)d\tau \quad y(t) = x(t) * h(t) \quad (\text{Convolution})$$

From digital signal processing theory, the output of any linear system is given by the convolution between the input and the pulse response of the channel.

Due to similarity between convolution and correlation, the above equation can be written as the cross correlation of both sides with the input  $x(n)$ .

$$R_{xy}(k) \approx \delta(k) * h(k) = h(k) \quad (\text{Cross-correlation})$$

The M Sequence used as input can be easily correlated to the received signal by the Fast Hadamard Transform, providing the desired channel impulse response (DeFerrari and Rogers, 2009). In case one already have the channel pulse response, the received waveform can also be obtained just inverting the operation as follows:

- $PR = FHT(\text{Waveform})$
- $\text{Received Waveform} = IFHT(PR)$

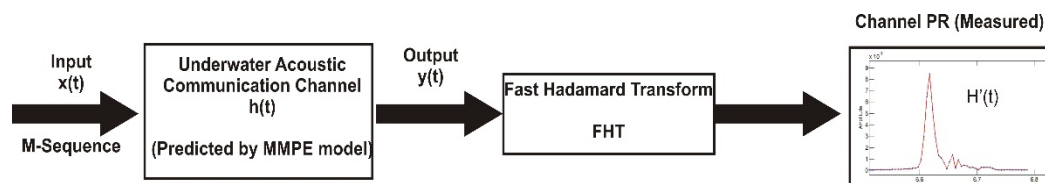


Figure 1.5: Channel PR measurement using M-sequences

### **Hyperslice Cancellation by Coordinate Zeroing (HCC0)**

The HCC0 is a method to eliminate multipath spreading and Doppler, using the remarkable property of perfect correlation of M sequences (Chang, 1992). The theory states that coordinate zeroing of compressed pulse eliminates the interference between the strong (M-Sequence) and weak signals (Message). DeFerrari and Rogers (2009) and DeFerrari and Wylie (2013) applied the HCC0 method in some previous experiments to eliminate Doppler interference from Doppler reverberation and direct pulse arrivals.

## **CHAPTER 2**

### **METHODOLOGY**

#### **2.1 MODELLING PARAMETERS**

The thesis is based on simulation results from MMPE model. Thus, the underwater acoustic channel must be modeled accurately to let MMPE provide reliable results. This way, the oceanographic environmental data from the research area were extracted from previous works from IEAPM and real data acquired at sea.

##### **Bottom Characteristics**

The majority of the sea bottom in the research area is classified as fine sand and the estimated sound speed is 1684 m/s (Simões et al, 2012). In addition, the sub bottom depth was defined as 1000m to avoid time delayed arrivals due to refraction of sound propagating through the bottom, keeping the focus on pulse reflections at boundaries and refractions in the water column.

##### **Bathymetry profiles and Source/Receiver depths**

The two modeled channels were flat, with zero bathymetric gradient, simulating a transmission along an isobathymetric contour. Further, the source and receiver were considered placed at the following depths:

- Channel 1- Depth: 50m, Sd=30m; Rd=15m;
- Channel 2- Depth: 200m, Sd=120m; Rd=60m;

## **Range**

The distance between the source and receiver for the numerical simulations were 10km for both channels.

## **Frequencies and Bandwidth**

The following center frequencies were used in the numerical simulations:

- 800 and 3200 Hz – 50m deep channel;
- 3200Hz – 200m deep channel.

Furthermore, all MMPE runs were done for both the center frequency  $f_c$  and a bandwidth of 25% of  $f_c$ . Therefore, one can analyze the estimated channel pulse responses and identify the multipath interactions by the arrival time.

## **Sound Speed Profiles**

This thesis results are based on SSP estimated from both data collected by sensors along a moored buoy in an approximate 50 m isobaths and some CTD data collected by a Brazilian Navy ship in the area.

### **➤ SSP from buoy data**

Along the years of 2013/2014, several oceanographic parameters such as temperature and salinity were recorded at a rate of 1 sample per hour, to monitor the upwelling events in the region of Arraial do Cabo-Brazil. The sensors were placed at the following depths: sea surface, 10, 15, 20, 25, 35 and 45m. However, data were linearly interpolated or extrapolated using available data from sensors to provide 5m resolution from the sea

surface to the bottom. Figure 2.1 shows some vertical temperature profiles (VTP) related to upwelling events that occurred during 2013-2014. For this thesis, the chosen VTP was observed in 2013 spring, from Oct 07<sup>th</sup> to Nov 17<sup>th</sup>.

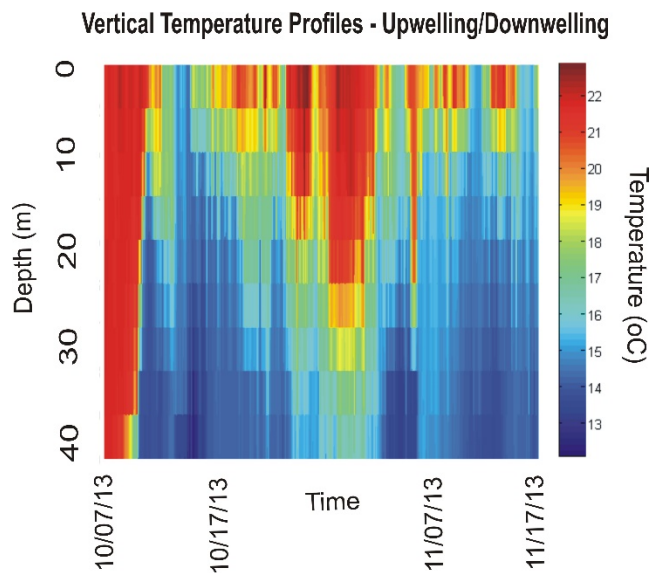


Figure 2.1: Vertical Temperature Profiles

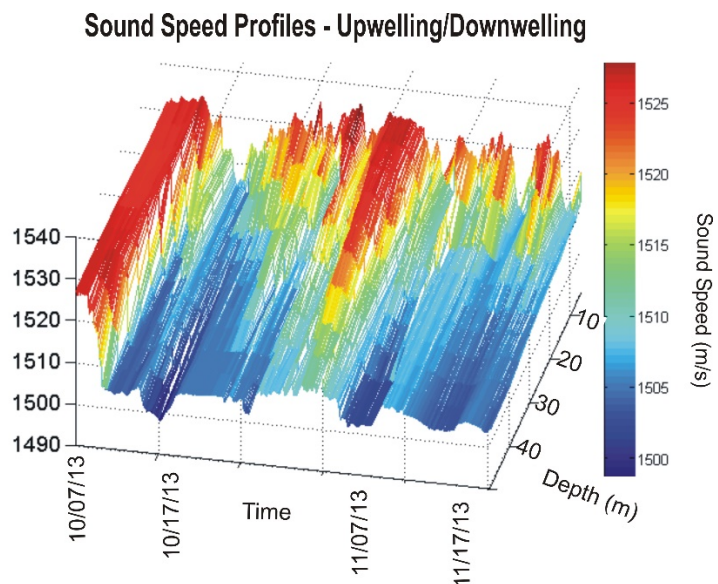


Figure 2.2: Sound Speed Profiles – Upwelling event

In figure 2.2, the sound speed profiles were calculated using the nine-term equation for the sound speed in the oceans (Mackenzie, 1981) as a function of previously interpolated temperature (T), salinity (S) and depth (D) as follows:

$$C(D,S,T)=1448.96 + 4.591T - 5.304 \times 10^{-2}T^2 + 2.374 \times 10^{-4}T^3 + \\ 1.340 (S-35) + 1.630 \times 10^{-3}D + 1.675 \times 10^{-7}D^2 - \\ 1.025 \times 10^{-2}T(S - 35) - 7.139 \times 10^{-13}TD^3$$

The sound speed profiles for the study of the temporal coherence were divided in 4 groups. Figure 2.3 shows the evolution of the SSP in 12 hours, for all cases. The first group, in red, shows an almost warm isothermal profile before the upwelling, in a SW/W wind condition. In green, the second group shows the occurrence of the upwelling itself, in a condition of NE/E wind at surface, expressed by a strong gradient in temperature profiles. The third group of SSP, in blue, looks similar to the first group. After the transition to upwelling, cold water fills the channel, as indicated by cold isothermal SSP, after the upwelling event peaks. The SSP in black were observed during the passage of internal tidal waves.

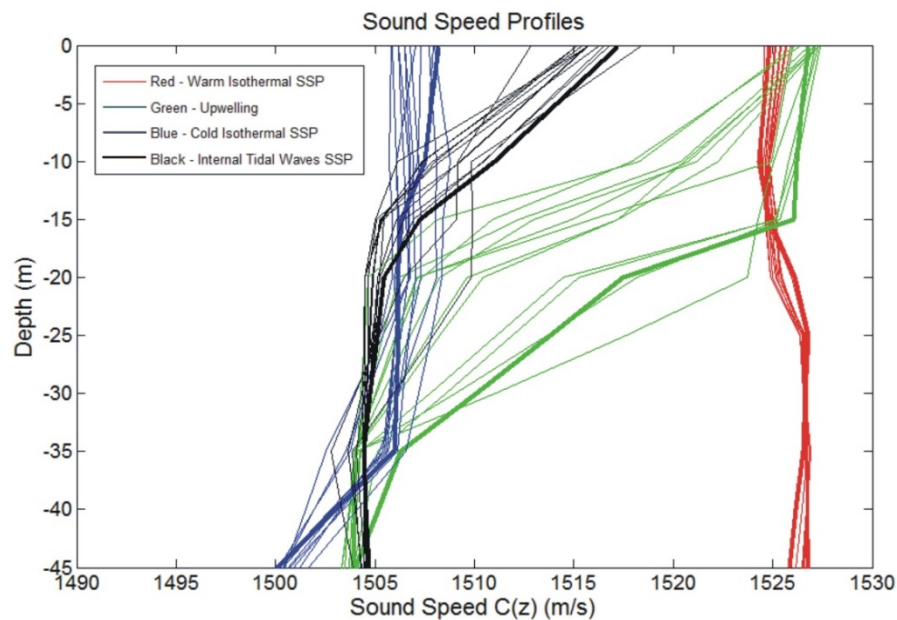


Figure 2.3: Evolution of Sound Speed Profiles in time



➤ **SSP from CTD**

For the analysis of the acoustic propagation in a 200m deep channel, the SSP were estimated based on some CTD data collected in an oceanic area near to IEAPM during the summer of 2006.

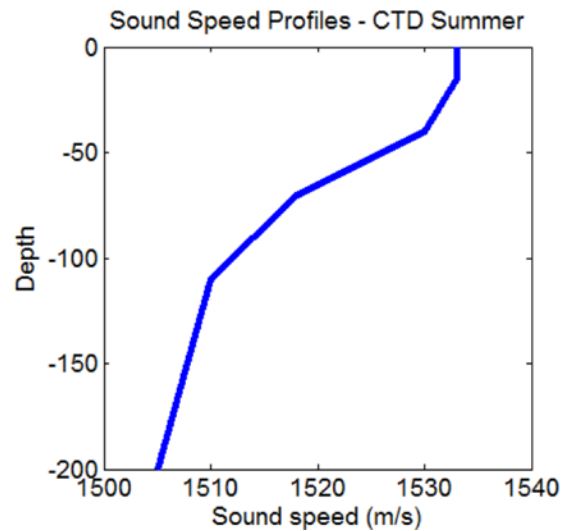


Figure 2.4: Sound Speed Profiles CTD (200m deep channel)

The curve in figure 2.4 was estimated based on an average of some SSP in the research area. The profile shows that, below the mixed layer (0-20m) where the sound speed is almost constant, the sound speed decreases continuously until the bottom of the channel.

## 2.2 DIGITAL COMMUNICATIONS SYSTEM

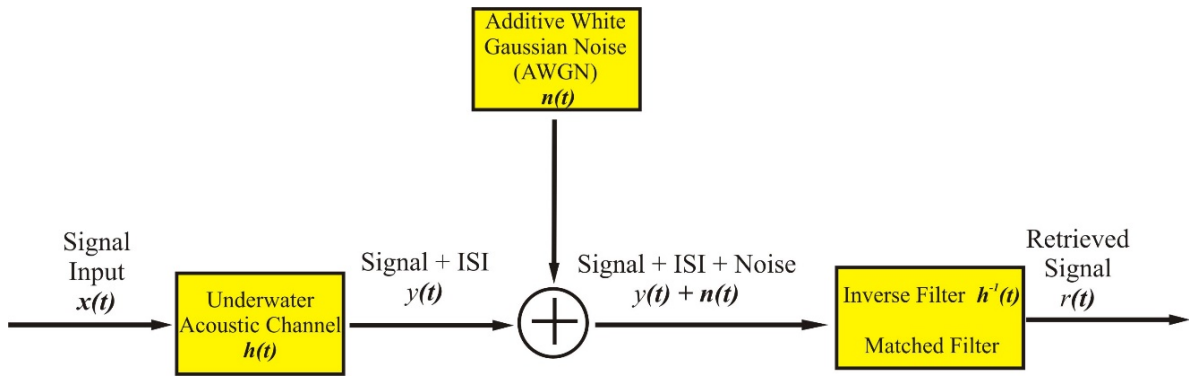


Figure 2.5: Digital Communications System

The block diagram in figure 2.5 represents a basic digital communications system to be simulated in this work, assuming two system properties: linearity and time invariance during short periods of time. Thus, the classic linear time invariant (LTI) approach can be used to generate the transmitted and received pulses through the system.

### Signal Input $x(t)$

In this thesis, the basic unit for any input signal is a “Bit”, defined here by four cycles of a continuous sinusoidal wave (CW) of the carrier frequency, sampled 4 times per cycle to avoid aliasing, represented by a total of 16 samples/bit. The system input, composed only by a sequence of bits, is phase modulated by the M-sequence code as follows:

$$x(t) = A \cos(2\pi f_0 t + b_k \Theta)$$

where  $f_0$  is the carrier frequency and  $b_k \Theta$  is the m-sequence modulation. The signal phase states can only assume 0 or  $\pi$  values, and depending on that, the bit can assume only two possible values: +1 or -1.

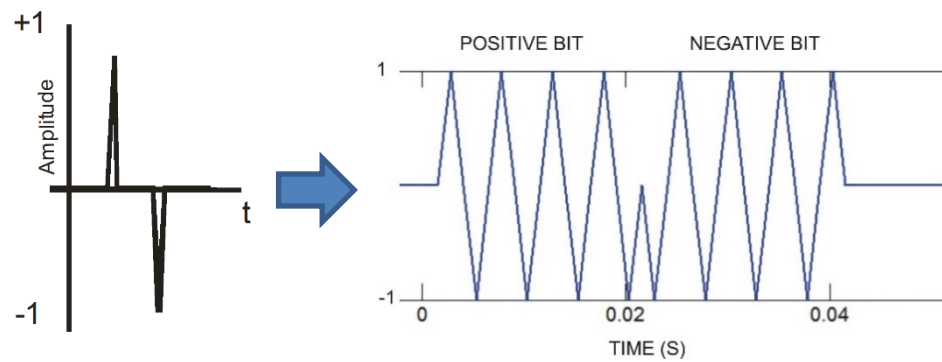


Figure 2.6: Left: a positive and negative bit (envelope).  
Right: bits represented by 4 cycle pulses, phase modulated

### Underwater Acoustic Channel $h(t)$

The UAC is represented by the channel pulse responses  $p(t)$  estimated from MMPE model, accounting for fading, multipath and reverberation phenomena which affects the signal propagation.

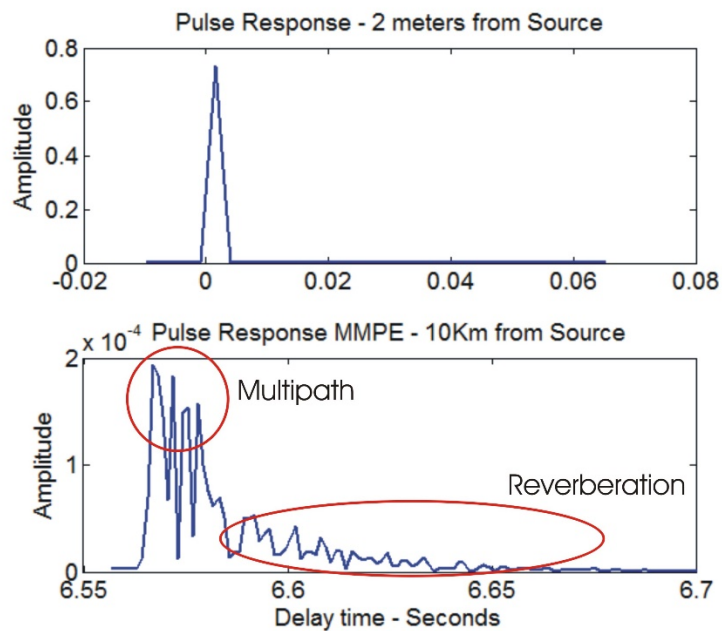


Figure 2.7: Above, a PR received close to the source. Below, the same PR received 10Km far from source, showing strong fading, multipath and reverberation

The pulse responses in time domain predicted by the MMPE model in figure 2.7 show clearly not only the interactions between the sound rays and the boundaries (multipath) but the reverberation caused by random phenomena. In this case, the source depth is the same of receiver depth, for a transmission in 3200Hz, and shows the fading in terms of pulse amplitude and pulse signal spread in time, going from 5ms for a receiver close to the source to about 100ms, for a receiver 10km far.

### Channel Output $y(t)$

In time domain, the response of the system  $y(t)$  can be simulated by the convolution between the signal input  $x(t)$  and the channel pulse response  $h(t)$ :

$$y(t) = \int_{-\infty}^{\infty} x(\tau)h(t-\tau)d\tau \quad , \quad y(t) = x(t) * h(t) \quad (\text{Convolution})$$

However, using the Fourier Transforms properties, the above convolution in time domain becomes a simple multiplication in frequency domain between the FFT of the input signal multiplied by the channel frequency response (FFT of  $h(t)$ ), as follows:

$$\begin{aligned} X(f) &= \int_{-\infty}^{\infty} x(t)e^{-i2\pi f t} dt \quad (\text{FFT } x(t)) \quad , \\ H(f) &= \int_{-\infty}^{\infty} h(t)e^{-i2\pi f t} dt \quad (\text{FFT } h(t)) \quad , \\ Y(f) &= X(f) \cdot H(f) \quad (\text{Output in frequency domain}) \end{aligned}$$

To transform back from frequency to time domain, one can perform the Inverse FFT of  $Y(f)$ , obtaining the same result as the original convolution above.

$$y(t) = \frac{1}{2\pi} \int_{-\infty}^{\infty} Y(f)e^{i2\pi f t} dt \quad (\text{Inverse FFT of the output } Y(f))$$

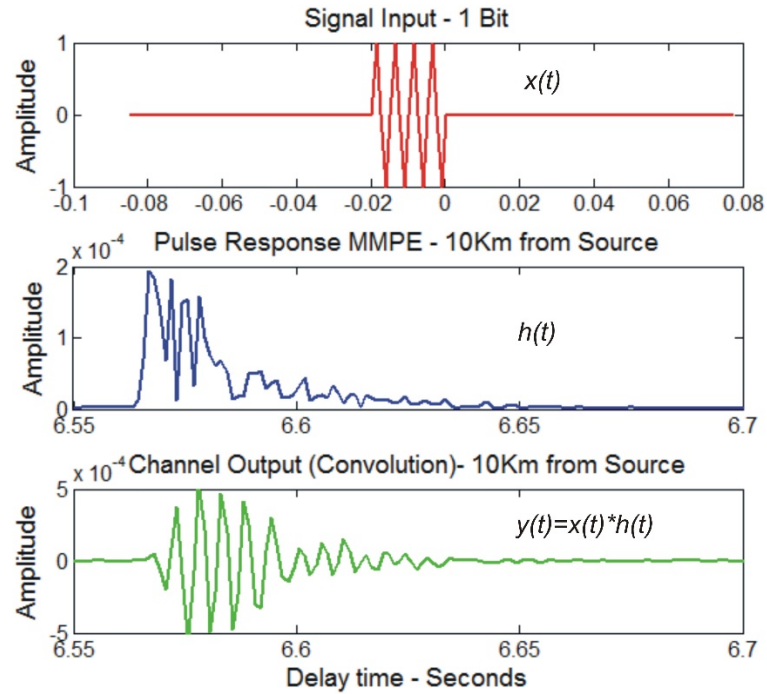


Figure 2.8: Simulation of 1 Bit propagating through the channel

In figure 2.8 one can visualize the simulation of a transmission of only 1 bit (3200Hz,  $S_d=R_d$ ) and verify how the original four cycle pulse was affected and distorted when travelling through the channel.

$$\mathbf{Output + Noise = } y(t)+n(t)$$

Noise is always present in communication channels and is the major impairment in many communication systems (Proakis and Salehi, 2008). So, to simulate a realistic channel, some Additive White Gaussian Noise (AWGN) must be applied at the receiver. The AWGN is a model used to simulate background noise presenting uniform power across the frequency band and normal distribution with an average in time domain of

zero. Typically, the relation between the Signal power and Noise power is given by the Signal to Noise Ratio (SNR), expressed in decibels.

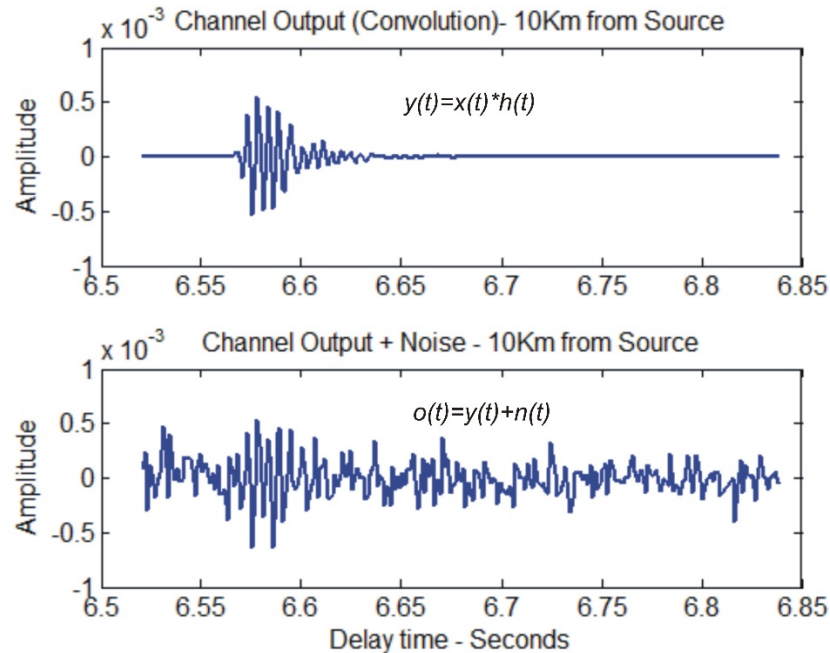


Figure 2.9: Above, 1 bit transmitted in a no noise environment. Below, in a noise environment (SNR -5db)

### Equalization

Defined as the process of reverse distortions incurred by a signal transmitted through a channel (Proakis and Salehi, 2008), the equalization is fundamental to improve any communication system performance. Underwater communication systems in shallow water must correct for multipath signal spreading to minimize inter-symbol interference and to recover the signal level from pulse spreading in time along the channel. Furthermore, there is always some background noise to complicate the retrieval of the original message. Therefore, equalization or filtering is vital to undo the distortions caused by the channel and restore the signal at the receiver through multipath

recombination. In this thesis, two filters, the inverse filter and the optimal matched filter, will be evaluated for signal retrieval.

### Inverse Filter

Proakis and Salehi (2008) stated that to reduce inter-symbol interference, the use of an inverse filter is required. Basically, the inverse filter is a deconvolution process that tries to undo the pulse spreading, and compensates for the distortions from multipath, restoring the original signal. The inverse filter transfer function  $G(f)$  is the reciprocal of the channel frequency response  $H^1(f)$  (Proakis and Manolakis, 1996), estimated from MMPE model and is usually performed in the frequency domain due to the convolution property of the Fourier transforms, cancelling the distortions, as  $H(f)*H^1(f)=1$ . Thus, the deconvolution in time domain becomes an inverse FFT of a simple division between two complex spectra in the frequency domain: the output + noise signal  $Z(f)=\int_{-\infty}^{\infty}(y(t)+n(t))e^{i2\pi ft}df$  and the channel frequency response  $H(f)$ .

$$R(f)=[Z(f)*H^1(f)] \text{ (frequency domain)} \quad r(t)=\int_{-\infty}^{\infty}R(f)e^{i2\pi ft}dt \text{ (time domain)}$$

However, in the presence of background noise, the inverse filter performance is poor, increasing noise low power frequency components compared to the high power frequency signal. Thus, for low signal to noise ratio (SNR), the inverse filter could be useless, as the noise could dominate the deconvolved signal in time domain.

In real experiments, the incoming M-sequences in noise should be band passed filtered to avoid aliasing, synchronously sampled, then averaged for about a minute to

increase SNR to let one measure the channel PR and inverse filtered for message retrieval.

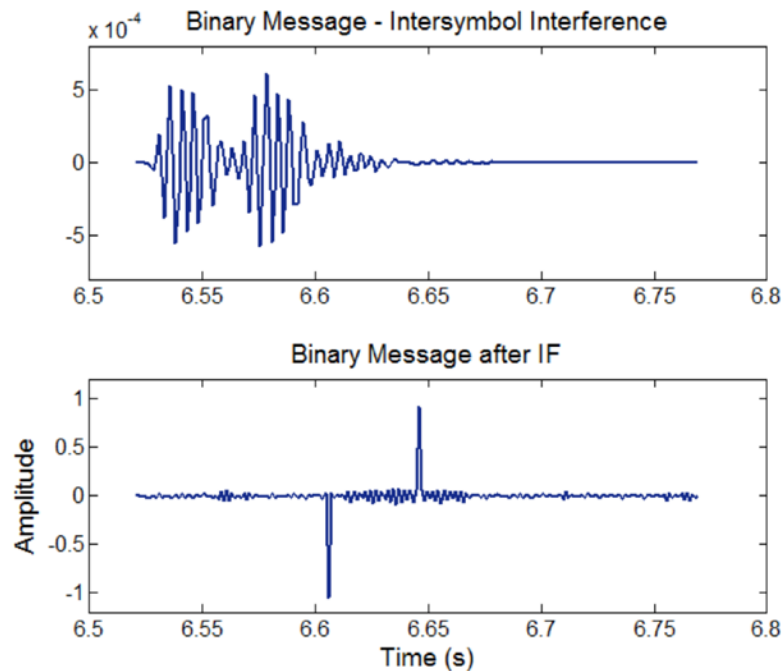


Figure 2.10: Transmission and Inverse filtering of 2 bits

Above in figure 2.10, 2 sequential bits at receiver, 1 positive and 1 negative, after propagating 10Km through a no noise channel with  $f_0=3200\text{Hz}$ , accounting for multipath and inter-symbol interference. Below, the inverse filter results, retrieving correctly the 2 original bits as desired.

### Matched Filter

Matched filters are often used in digital communications to detect transmitted signals in the presence of background noise. Considered the “Optimal Filter”, the matched filter maximizes the signal to noise ratio (SNR) and is easily performed cross correlating the received signal and the channel pulse response in time domain:



$$r_x = y(T) = \int_{-\infty}^{\infty} r(\tau)x(\tau) d\tau \quad (\text{Cross-correlation})$$

However, to let the receiver correctly estimate the symbol in the correlated message, the sequence will be sampled (16 samples/bit) and compared to a threshold as follows:

sample > 0 → Bit positive +1

sample < 0 → Bit negative -1

## 2.3 METHOD TO IMPROVE UW DIGITAL COMMUNICATIONS

Using the previous background about the digital communications systems, a unique method to optimize the underwater communications in shallow waters is presented here to directly measure and update the channel pulse response using M sequences while collecting the message, simultaneously. The method involves several intermediate steps described as follows:

- Creation of the bit streams to be transmitted through the channel
- Simulation of a transmission through the Underwater Acoustic Channel
- Pulse compression by Hadamard transform and Channel PR measurement
- Hyperslice Cancellation by Coordinate Zeroing (Chang,1992)
- Inverse Hadamard Transform
- Matched Filtering

### **Creating the bit streams to be transmitted through the channel**

The binary stream to be transmitted is created from a summation, sample by sample, of two other binary sequences of same length: a M-sequence and a Message. However,

the M sequence amplitude is several times greater than the amplitude of the message. The idea here is to spread a weak signal (Message) along the strong signal (M-sequence) to take some advantage of the post-processing method based on pulse compression using Hadamard transforms, as to be stated later. In figure 2.11, the amplitude of the M-sequence is 2 times greater than the message, producing a bit stream composed of amplitudes oscillating between 5 and 15 after the summation.

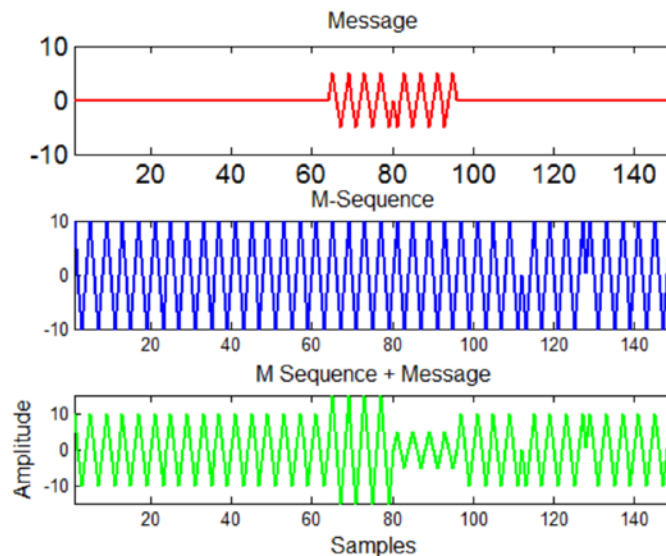


Figure 2.11: Bit stream components

### **Simulating a transmission through the Underwater Acoustic Channel**

According to previously stated modeling parameters, the simulation is performed by the convolution between the binary stream (Mseq+Message) and the channel pulse response from MMPE model, as exemplified in figure 2.8. Both M-Sequence and Message were composed by 2047 bits, sampled 16 times/bit.

### Pulse compression by Hadamard transform and Channel PR measurement

In this step, the previously simulated bit stream transmitted through the channel is pulse compressed by the Fast Hadamard Transform providing the measured channel pulse response. Due to M sequences and FHT properties, the FHT compress the M-sequence energy contained on the received bit stream in the first part of the channel response (Bjor, 2000), increasing the SNR in  $10 \cdot \log_{10}(P)$  decibels, letting the original message several times smaller in amplitude spread over the remaining length of the sequence.

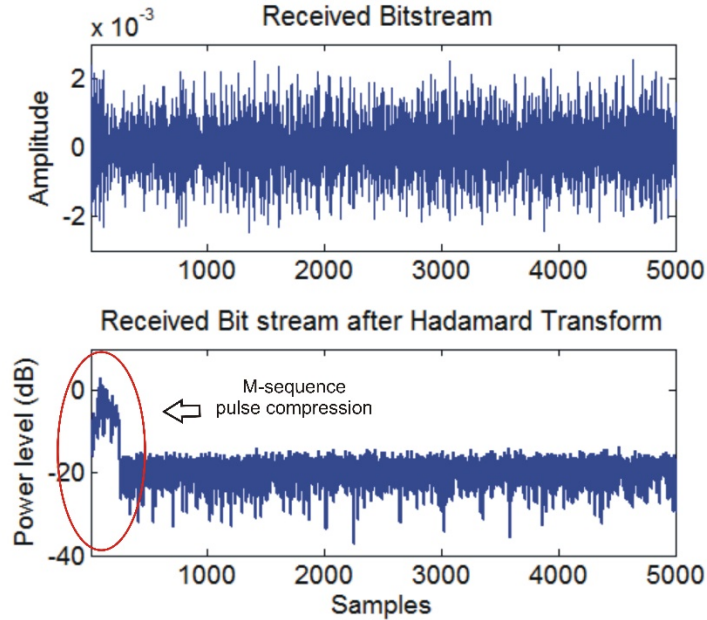


Figure 2.12: Energy pulse compression by FHT

### Hyperslice Cancellation by Coordinate Zeroing (Chang,1992)

The HCC0 method eliminate the interference between the M-Sequence and the Message, zeroing the peak of energy in the measured pulse response, letting only the weak Message spread over the remaining length of the sequence.

### Inverse Hadamard Transform

After the coordinate zeroing, an inverse fast hadamard transform uncompress the weak signal from the pulse response sequence. However, as it is still buried in noise, some filtering is fundamental in the process, to correctly retrieve the original binary message.

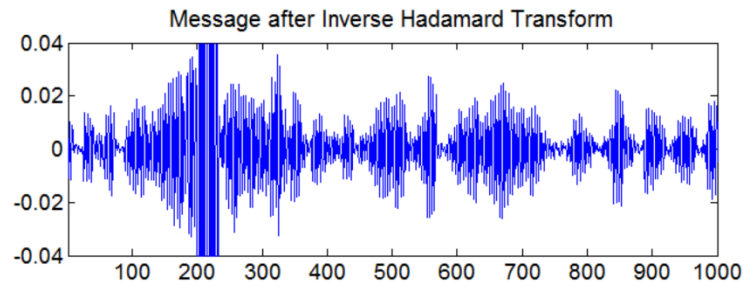


Figure 2.13: Message in noise after FHT

### Matched Filtering

As the simulation is done using some background noise added to the transmitted sequence, the retrieved signal after the IHT in step 5 is still not the original message. Thus, the signal is matched filtered with the pulse response measured in step 3. Here, both signals are cross correlated and the result is sampled at a rate of 16 samples/bit. Assuming perfect synchronization, at each time of detection or at steps of 16 samples, the matched filtered samples values are compared to a threshold value to decide the bit polarity. This way, the bit is considered positive if the sample is greater than zero and negative if less than zero.

Bit +  $\rightarrow$  sample at time of decision  $> 0$ ;

Bit -  $\rightarrow$  sample at time of decision  $< 0$ ;

## **CHAPTER 3**

### **TEMPORAL COHERENCE AND THE INVERSE FILTER REFRESH TIME**

In this chapter, results of a shallow water acoustic propagation simulations are analyzed and compared, in terms of temporal coherence of the transmitted message and the inverse filter refresh time, for several ocean temperature conditions.

Ocean is classified by researchers as a very complex environment for the transmission of communication signals. Further, the research site presents energetic oceanography fluctuations due to the significant upwelling events, leading to severe distortions of the average sound speed profiles in depth and time.

#### **Effects of Upwelling on SSP**

Before the beginning of an upwelling event, the wind blows from S/SW, bringing warm surface waters from the sea to shore, inducing a weakly stratified mixed layer from the surface to the bottom, presenting warm isothermal / vertical sound speed profiles.

However, as soon as the wind changes its direction, and blows from N/NE, the channel properties begin to change their characteristics, i.e., temperature and salinity for all depths. Thus the sound speed profiles became rapidly time variant passing from an almost constant vertical profile to a profile with strong gradient. Furthermore, the stratification increases as the upwelling phenomena continues leading to a final condition of a cold shallow water channel expressed by a slightly sound speed profile anomaly.

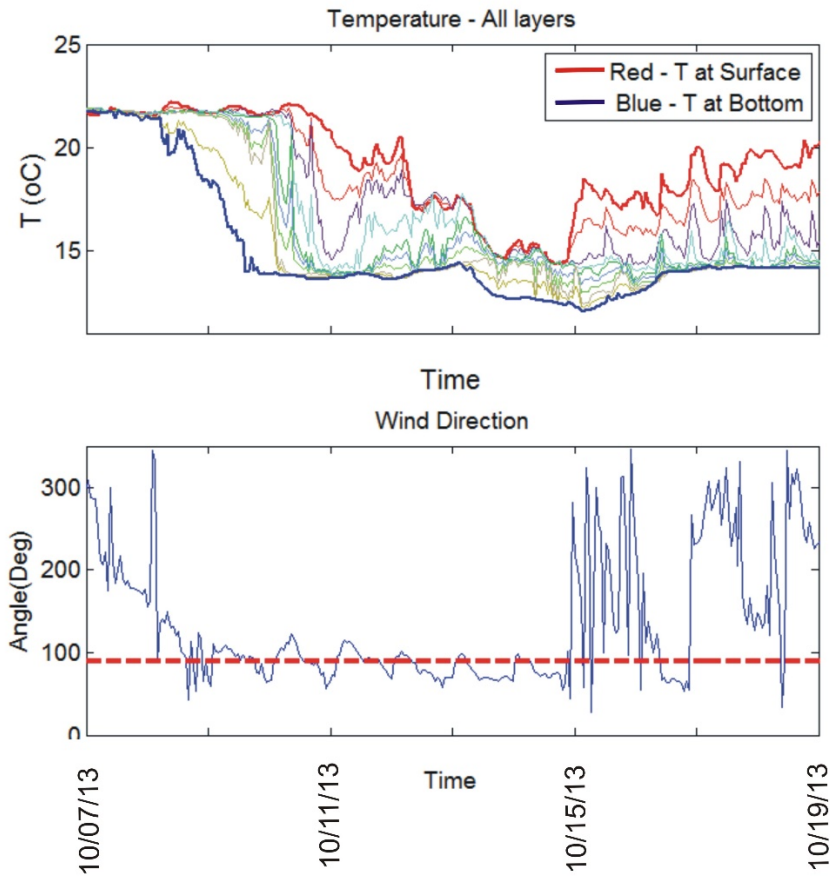


Figure 3.1: Above, temperature time series for each thermistor depth. Below, the red dashed line highlights wind direction for upwelling occurrence.

In figure 3.1, one can compare the relation between the temperature distribution for all thermistors depths and the wind direction, for a period of 12 days, covering main ocean temperature conditions:

- isothermal warm;
- upwelling;
- isothermal cold;
- internal tidal waves.

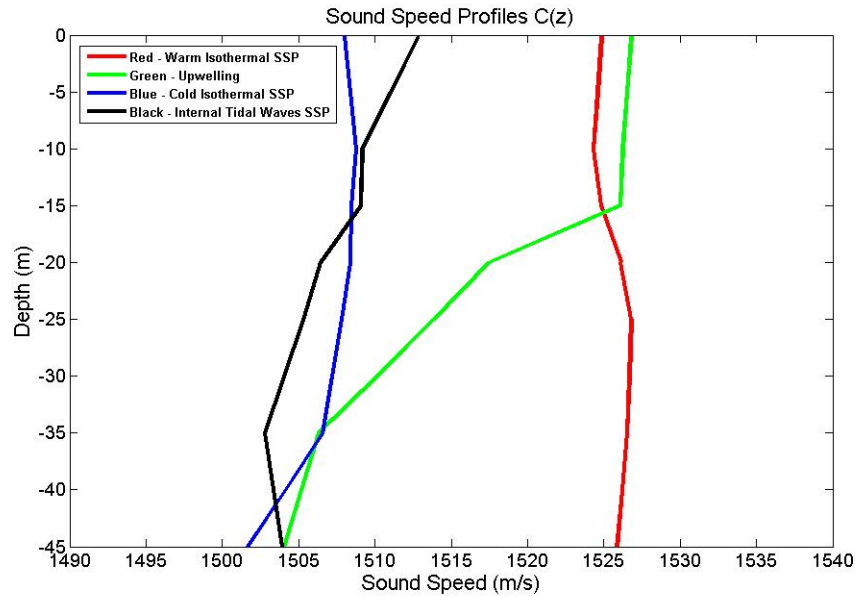


Figure 3.2: Sound Speed Profiles for different ocean temperature conditions

Next, the effects of the changing SSP from upwelling on channel pulse response will be predicted using a propagation model. The results presented in this chapter are from several runs of MMPE model, for a 10 Km long and 50m flat bathymetry propagation channel, based on temperature and sound speed profiles retrieved from the buoy sensors for a “experimental time” of 12 days, in the end of the fall of 2013.

The source depth is 30 meters and receiver is located 15 meters deep, halfway between the source and the sea surface. For this work, only one range-independent SSP estimated from the buoy sensors will be used in the model. The simulations in the MMPE model will be performed for a low and a high frequency: 800 and 3200Hz, respectively, and for a bandwidth of 25% of these frequencies for all four SSP anomaly types mentioned above.

### **Temporal Coherence**

The objective of the MMPE model run is to predict how long the channel remains coherent. Based on theory from chapter 2, the temporal coherence will be calculated correlating channel pulse responses estimated from MMPE model runs, for several SSP's. The pulse responses show the interaction of the acoustic field with boundaries, surface and bottom, for each depth, leading to multipath propagation which is responsible for the inter-symbol interference between consecutive bits transmitted through the channel. Due to MMPE characteristics, an array of 90 rows (depth) by 256 columns (range) were created for each run. Then, the row number 19 of the array, representing the receiver depth (15m) was picked up and used in calculations.

The 1-hour resolution original data could not be inserted in the model directly due to the typical coherence time scale of only a few minutes in the ocean. Thus, intermediate SSP were interpolated in steps of 1 minute, and inserted in the model, providing estimated pulse responses to calculate the coherence. Also, the results were averaged over a band of 5 meters around the receiver depth, to provide reliable results of coherence time. The predicted pulse responses of the propagation channel are used to estimate the inverse filter refresh time. During good propagation conditions, the coherence time is typically long and so is the inverse filter refresh times are also long. This means that the original pulse response is still good enough to resolve the inter-symbol and to retrieve the original information. Conversely, every time the ocean temperature and SSP change rapidly, temporal coherence decreases, leading to short inverse filter refresh time to keep up with these fast real time varying sound speed profiles.



To check the kernel filter refresh time, a 4 cycle pulse is convoluted to the channel pulse response from MMPE model, for the initial time (minute 00) generating a simulated pulse transmitted through the channel. Then, for time delayed pulse responses for subsequent 01, 03, 05 and 10 minutes , a new pulse is simulated and used as an inverse filter to retrieve the original message.

The goal of this chapter is to understand the relationship between the temporal coherence and the refresh time of an inverse filter for idealistic acoustic propagation conditions, in a no noise environment, by comparing the modeling results for typical ocean temperature events in the study area.

### **3.1 – ANALYSIS OF COHERENCE AND INVERSE FILTER PERFORMANCE**

#### **Isothermal Sound Speed Profiles – Warm and Cold**

There are two situations in which the shallow water channel remains isothermal. The first is identified as a warm isothermal ocean condition which exists before the beginning of the upwelling event. The second situation happens right after the end of the transition from the previous warm to a cold isothermal distribution. Basically, the sound speed profiles are very similar, presenting almost vertical gradients for long periods of time. Therefore, as the temporal coherence and the inverse filter refresh time are directly related to the SSP gradient, one can expect similar coherence and filter performance.

In both cases, warm and cold isothermal SSP, the channel pulse responses express the particular way the acoustic waves interact with boundaries, refracting and reflecting along the channel for each ocean temperature condition. The main and strongest direct

arrival is generally surrounded by several RBR and surface reflections causing the pulse spread in time and change in wave phase.

### 800Hz

Comparing the phase and wave forms for minutes 00, 05 and 10 in each situation, one can check that the waves remain in phase and show approximately the same form during this period of time.

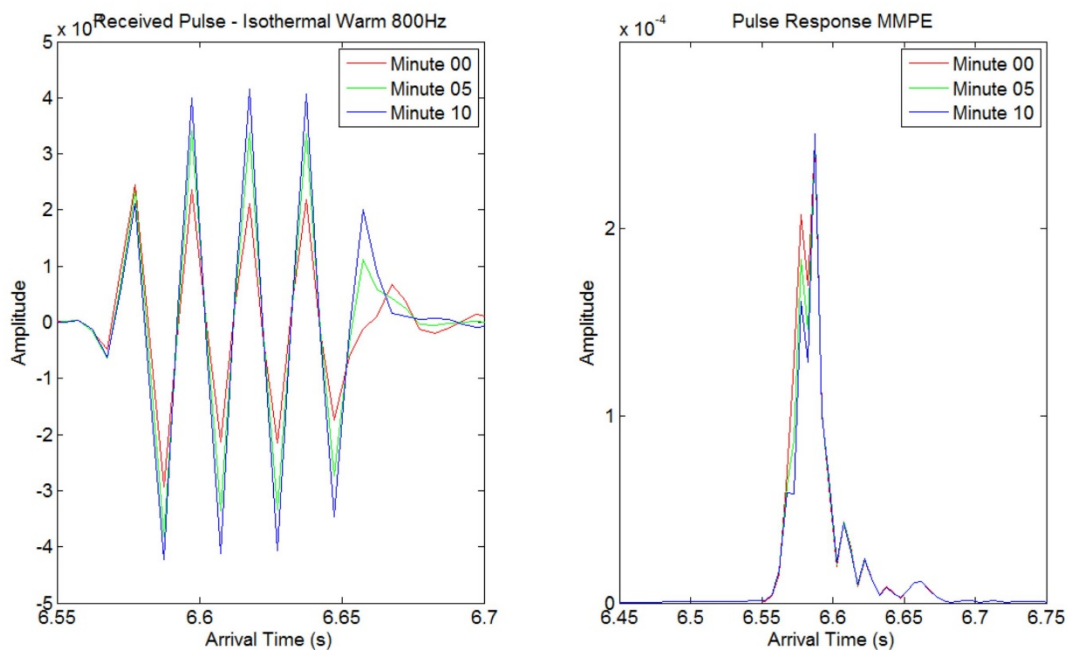


Figure 3.3: Received pulse and predicted Pulse Responses – Iso Warm SSP - 800Hz

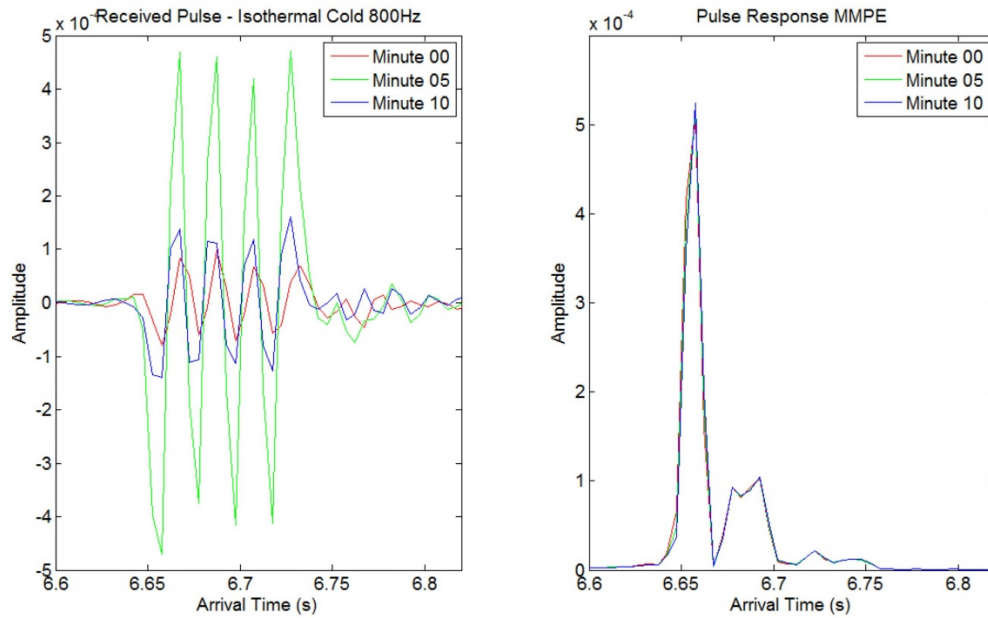


Figure 3.4: Received pulse and predicted Pulse Responses – Iso Cold SSP - 800Hz

Therefore, in an isothermal ocean condition, warm or cold, the temporal coherence is high and the performance of the inverse filter is good for several minutes, retrieving correctly, even in amplitude, the original message as the pulse responses remain in phase during this time. However, as the inverse filter PR becomes distant in time from the transmitted message, its performance degrades, showing that it is time to refresh the kernel of the filter to keep up with the environmental time changes (Figure 3.5).

## Isothermal WARM SSP – 800Hz

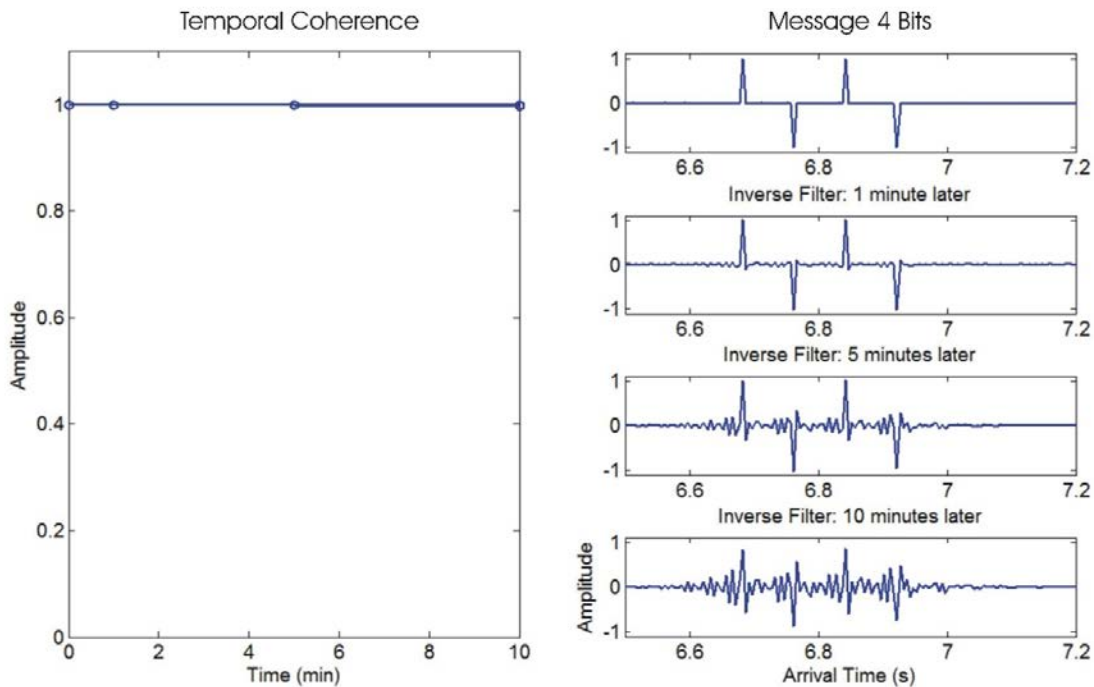


Figure 3.5: Temporal Coherence and Inverse Filter – Iso Warm SSP - 800Hz

## Isothermal COLD SSP – 800Hz

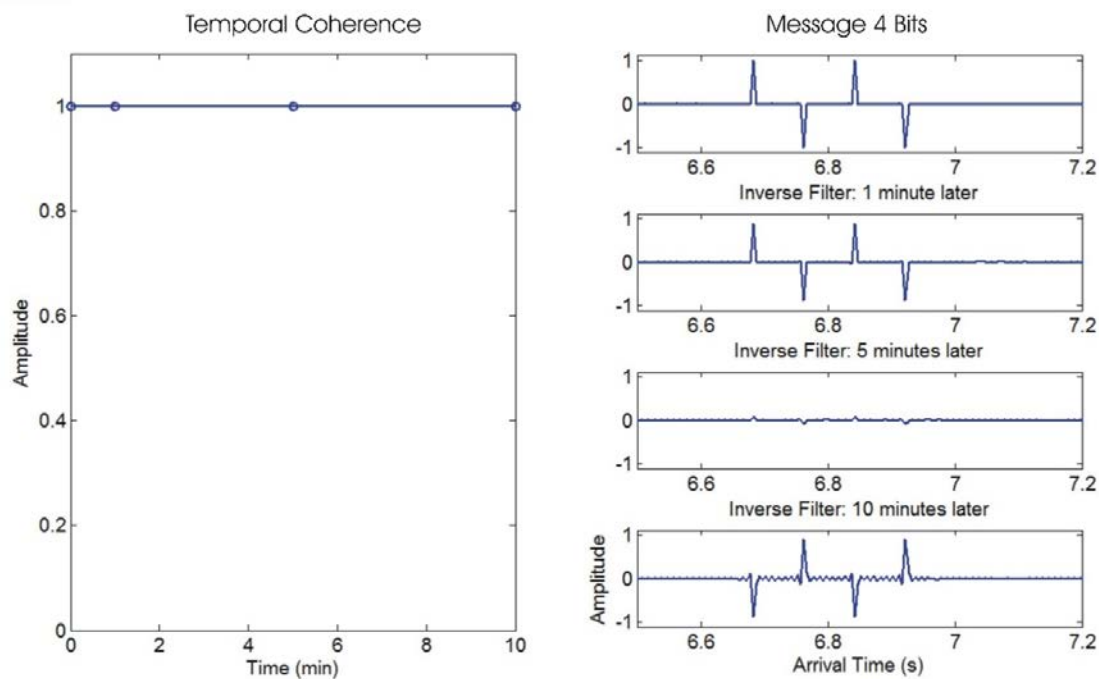


Figure 3.6: Temporal Coherence and Inverse Filter – Iso Cold SSP - 800Hz

### Deterministic x Random variation in the PR

Some fluctuations are deterministic and so can be recovered in theory. Other fluctuations are random and cannot be reliably predicted with propagation models.

In figure 3.6 an interesting phenomena happens in which the coherence remains high but the retrieved message is  $180^\circ$  out of phase suggesting the occurrence of a deterministic slow phase time shift of undistorted waveform and not a real loss of coherence due to random and unknown reasons as in a real ocean.

### 3200Hz

Bits or symbols travelling in high frequency typically suffer higher attenuation and inter-symbol interference. Thus, even in isothermal SSP conditions, signals simulated at 3200Hz show wave form and phase change in time, much faster than for 800Hz, as observed below.

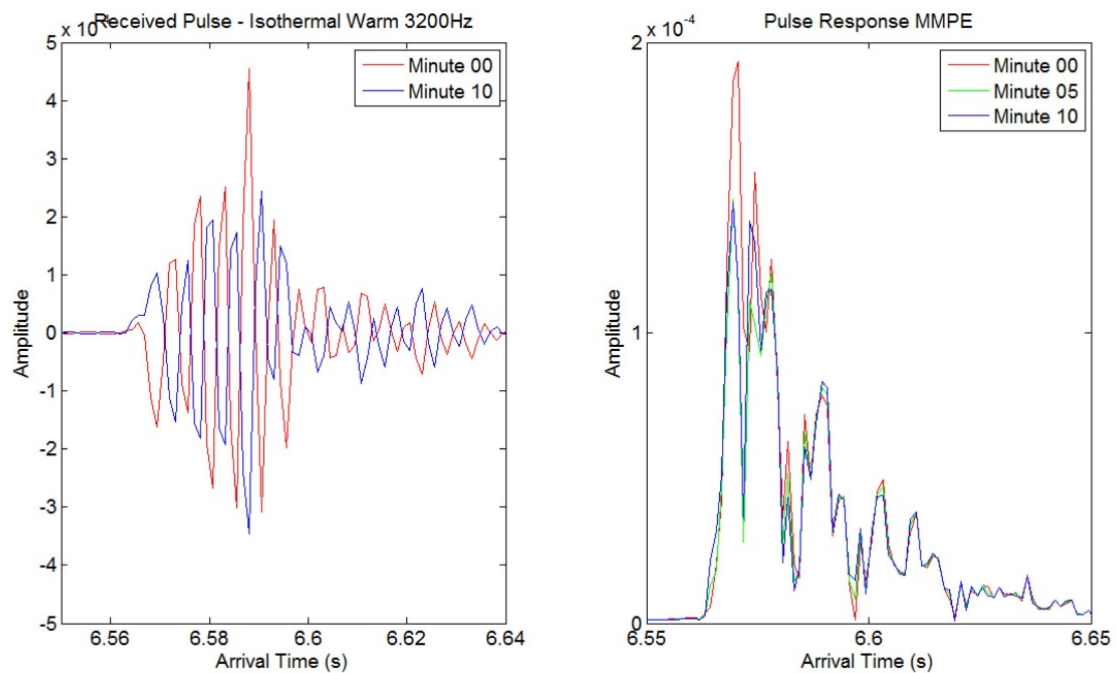


Figure 3.7: Received pulse and predicted Pulse Responses – Iso Warm SSP - 3200Hz

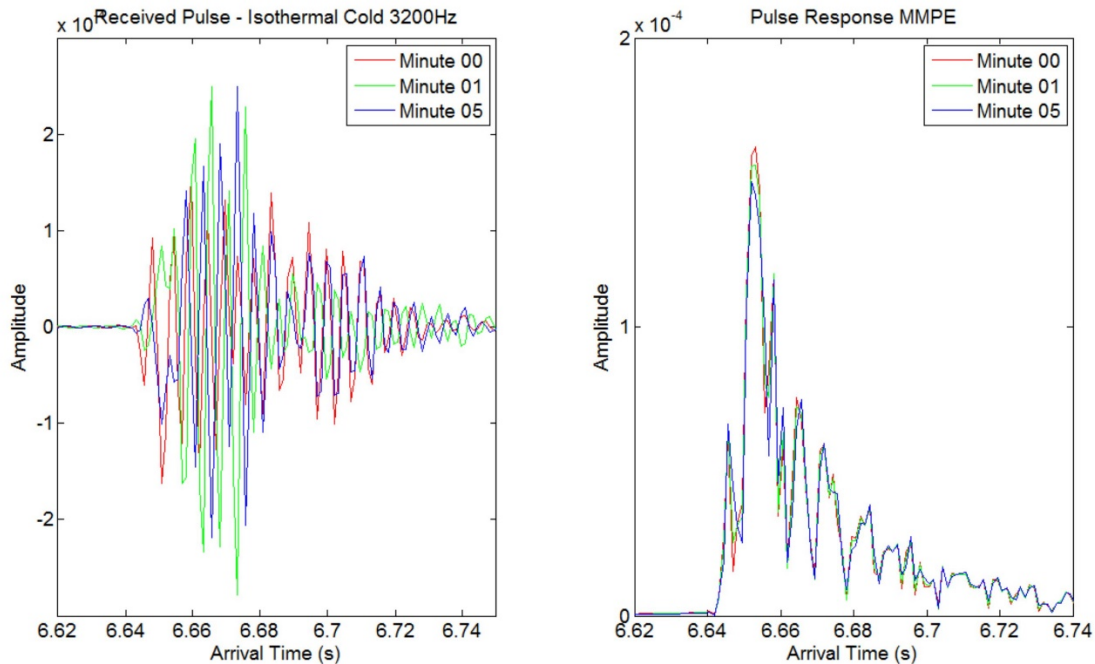


Figure 3.8: Received pulse and predicted Pulse Responses – Iso Cold SSP - 3200Hz

Also, the pulse responses present a reverberation phenomenon, a non-coherent part of the signal. Thus, the retrieval is correct for 1 minute only, being  $180^\circ$  phase reversed at 10 minutes. Urick (1983) suggests, the signals travelling at higher frequency, in this case 3200Hz, suffer stronger attenuation than those of 800Hz, as one can observe comparing the amplitude for both retrieved signals. For a transmission in these propagation conditions, one could probably recover the message just correcting for these time shift between signals in this 10 minute time frame. However, after 10 minutes, the signal suffers not only a time shift but loss of coherence due to some other random ocean fluctuations making the signal not recoverable anymore.

### Isothermal WARM SSP – 3200Hz

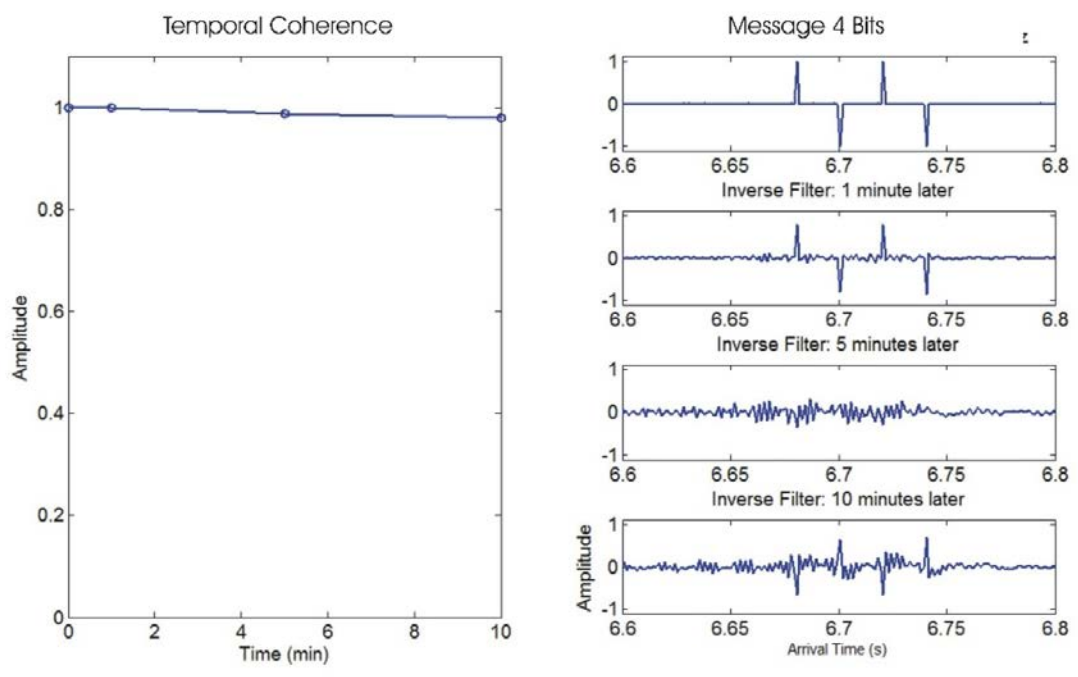


Figure 3.9: Temporal Coherence and Inverse Filter – Iso Warm SSP - 3200Hz

### Isothermal COLD SSP – 3200Hz

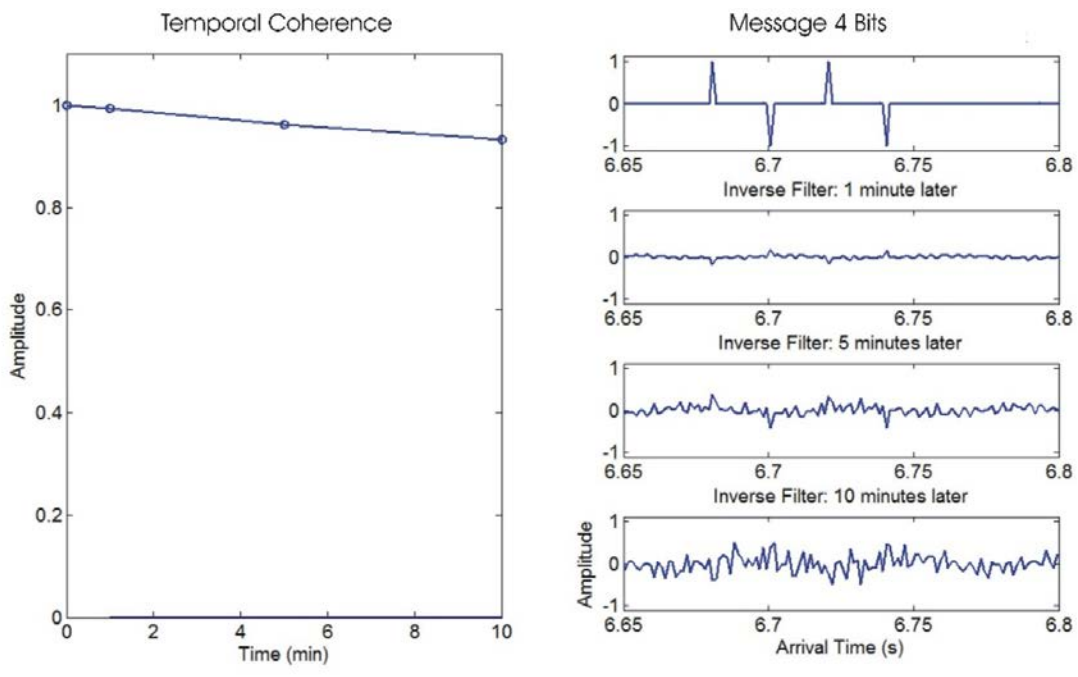


Figure 3.10: Temporal Coherence and Inverse Filter – Iso Cold SSP - 3200Hz

## **Upwelling Sound Speed Profiles**

### **800/3200Hz**

From a warm ocean temperature distribution, as soon as the wind changes its direction, blowing from N/NE, the channel begins to change gradually its characteristics, i.e., temperature and salinity for all depths, influencing deeply the sound speed profiles which became fast time variant passing from a vertical to a negative gradient. The SSP are one of the most important factors over the acoustic propagation, orientating the way rays refract along the channel and so the propagation itself.

The analysis of the temporal coherence and the inverse filters behavior during the upwelling event may help one to understand the impact of these events in underwater communications, especially in shallow waters. In this more interesting case, one can expect that the phase and wave form of 800 and 3200Hz channel pulse responses change rapidly in time due to the fast time varying sound speed profiles.

For a 800Hz simulation, one can observe in figure 3.11 that just some minutes later, the pulse response is already  $180^\circ$  out of phase, much faster than the previous case. Furthermore, the retrieved wave amplitude is around one order of magnitude lower than the original one meaning that the acoustic waves are attenuated in a different way, mainly due to the interactions at boundaries and reverberation.



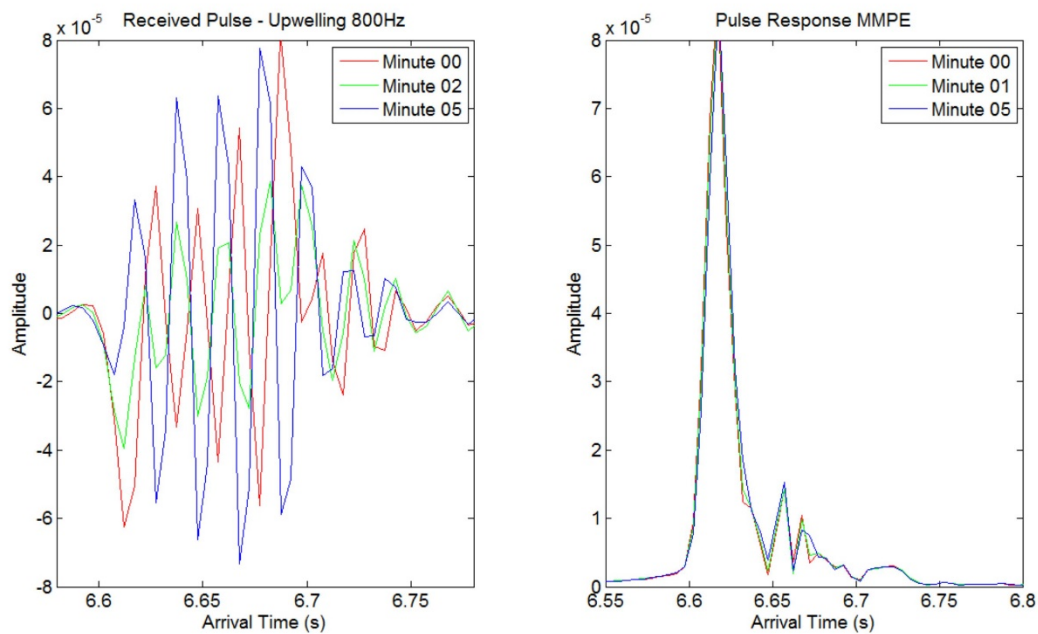


Figure 3.11: Received pulse and predicted Pulse Responses – Upwelling SSP - 800Hz

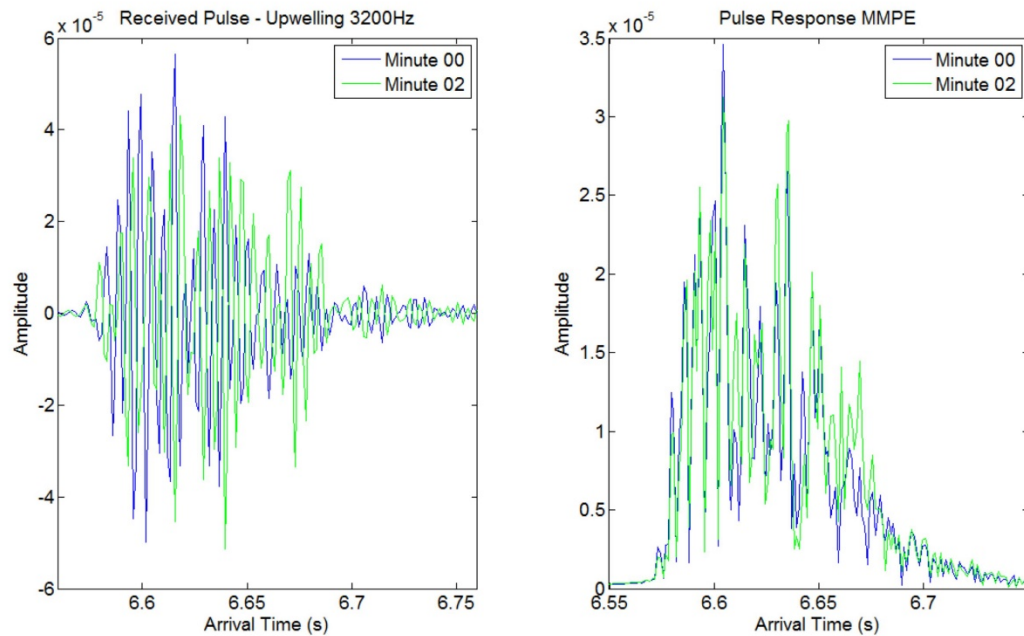


Figure 3.12: Received pulse and predicted Pulse Responses - Upwelling SSP 3200Hz

Therefore, the signal remains coherent enough to retrieve the message for only a few minutes, around 2/3 minutes. There is no phase shifting in time. As the time passes-by, the coherence decreases probably due to some random phenomena out of the scope of this work, making the signal unrecoverable. At this point, the inverse filter degrades its performance, not retrieving the message, as the pulse responses for minute 05 is totally different of minute 00, not only in phase but also in amplitude values along the pulse time of arrival.

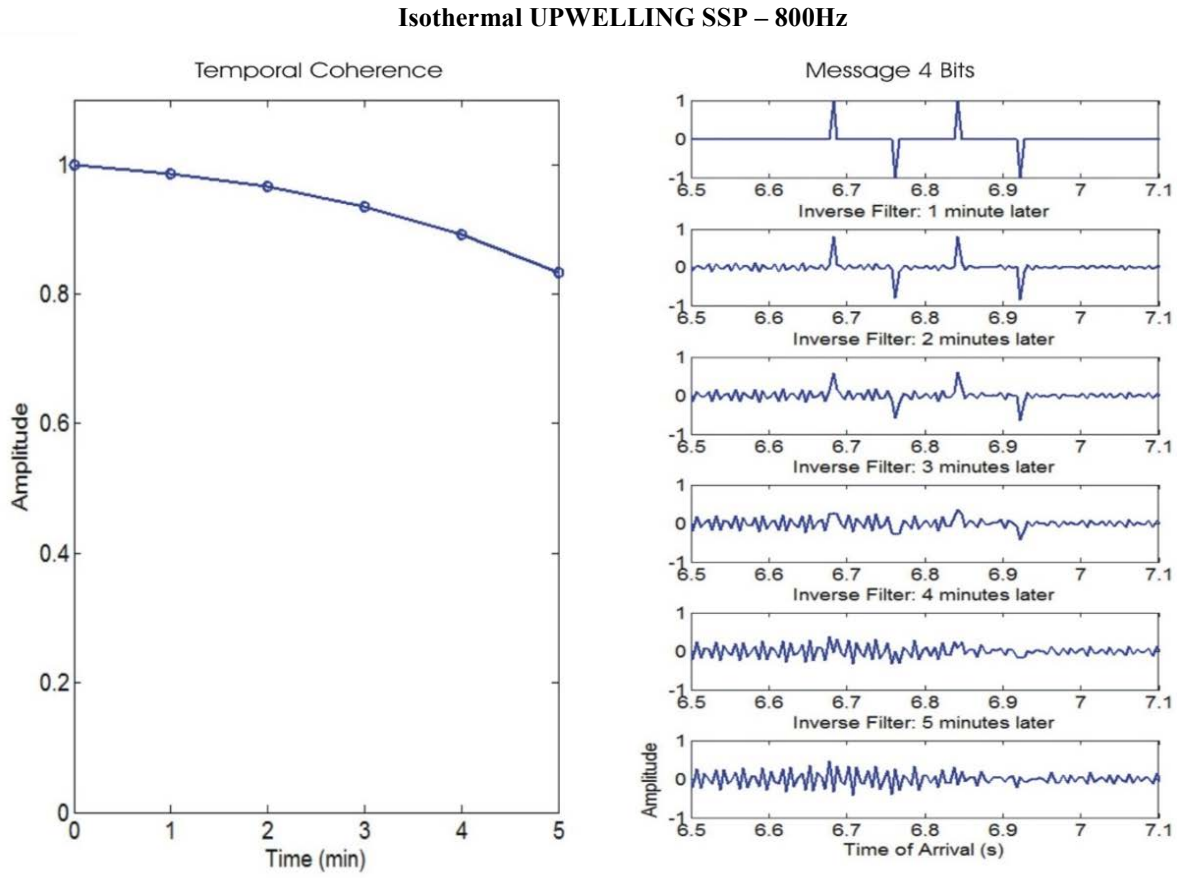


Figure 3.13: Temporal Coherence and Inverse Filter 800Hz - Upwelling SSP

### Isothermal UPWELLING SSP – 3200Hz

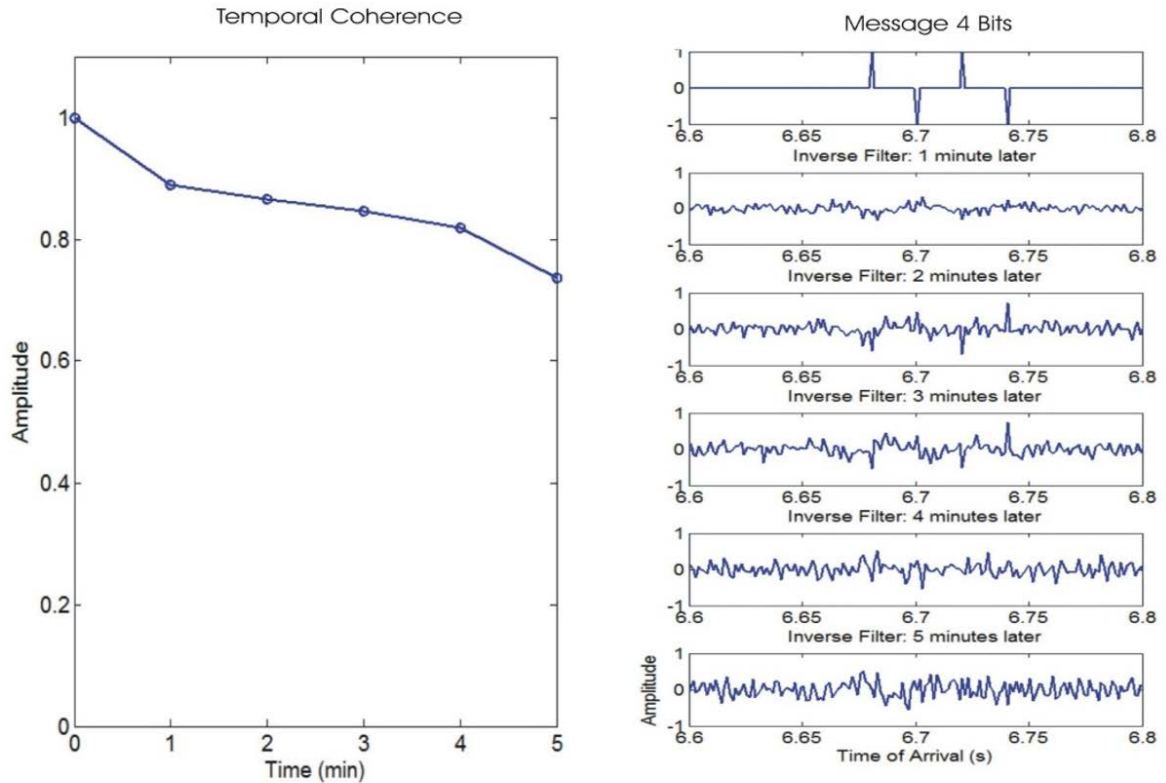


Figure 3.14: Temporal Coherence and Inverse Filter 3200Hz - Upwelling SSP

In figure 3.14, the signal decorrelates much faster than the 800Hz wave. The pulse responses from MMPE in figure 3.12 shows numerous interactions with boundaries, much more than for 800Hz for upwelling or the previous cases in a warm isothermal condition. In this case, one can observe that the interactions and so the pulse responses are much different for minutes 00, 02 and 05 due to the fast time varying SSP. The phase shifts for the first 3 minutes still keep the coherence high enough to retrieve a 180° phase shifted message. However, the loss of coherence after 3 minutes is also affected by the noise in the MMPE model calculations, interfering with the final result. At this point, the

inverse filter is not able to retrieve any message becoming useless pointing that it is time to refresh the filter to keep up with these ocean fluctuations.

### **Internal Waves**

In shallow waters, the presence of internal waves is usually the dominant problem for acoustic communications, as it induces oscillations of thermocline and by consequence the SSP, affecting the propagation. Internal waves are highly nonlinear waves, defined as gravity waves travelling through the interface between two water layers of different densities, transporting momentum and energy (Massel, 2015). Typically, their periods vary from several minutes to hours with frequencies oscillating between the inertial frequency  $f$ , around 14h for a latitude of 22°S, and the Brunt-Vaisala  $N(z)$  frequency.

$$f^2 < \omega^2 < N^2(z)$$

According to DeFerrari et al. (2008), from the temperature data, one can calculate ETA2,

$$\eta' = T' / dT / dz$$

related to the internal wave potential energy, for an acoustic field,

$$PE = (\rho / 2) N^2 \eta'^2$$

where  $T$  is the temperature perturbation in time and  $dT/dz$  is the vertical temperature gradient.

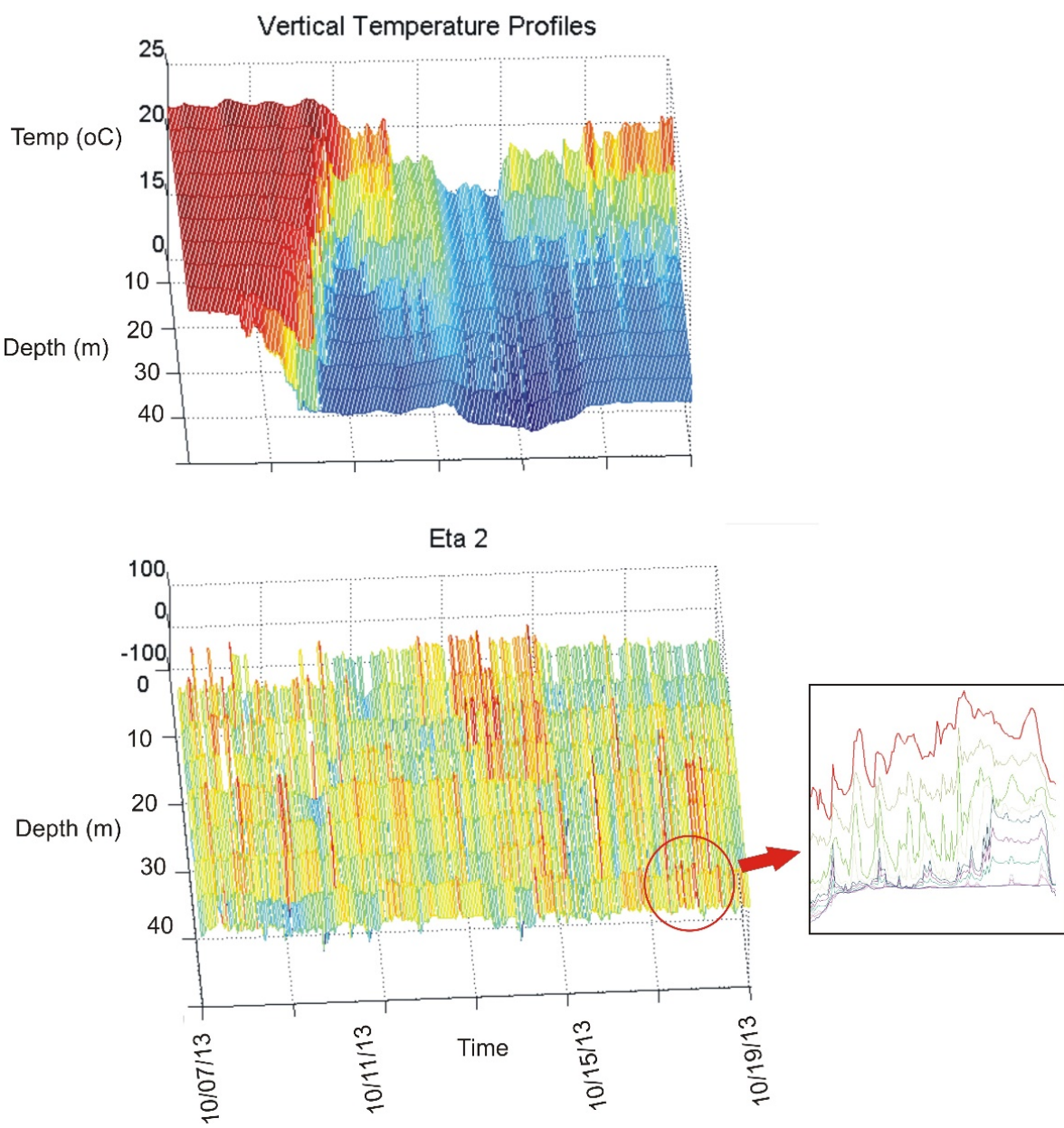


Figure 3.15: Vertical temperature profiles aligned in time to internal tides potential energy. In red circle, some internal tidal events.

Due to the 1 hour resolution of data retrieved from the buoy sensors, short period internal waves which occurred between two samples of temperature/salinity, could not be detected. However, some distortion to the SSP were observed during a downwelling event, with periods around 12h, probably related to the semi-diurnal tides, as shown in

figure 3.15. These waves called Internal Tides play a secondary role in the propagation channel compared to SSP distortions caused by the upwelling. In the research area, the ocean temperature distribution is most influenced by the upwelling events related directly to the wind direction in the area, not to internal tidal waves which could not be observed regularly in the data. Comparing the vertical temperature profiles to the ETA2 in figure 3.15, one can check that most peaks of potential energy are related to internal tides, which is highlighted in the red circle.

### **800/3200Hz**

For 800Hz, as in the upwelling event, in which there is a strong temperature gradient, the phase decorrelates in just a few minutes as one can verify comparing the channel pulse responses. In the 3200Hz case, not only the wave decorrelates but an additional reverberation complicates the inverse filter job. These results point to low temporal coherence and poor filter results, suggesting one to refresh the kernel of the filter.

During the internal tides, the signal phase remain coherent for only some minutes for 800Hz and around 1 minute for 3200Hz. To validate the coherence, one can compare it to the inverse filter performance, verifying that the kernel of the filter must be update in about 1 minute, in order to keep the communication system working as expected.

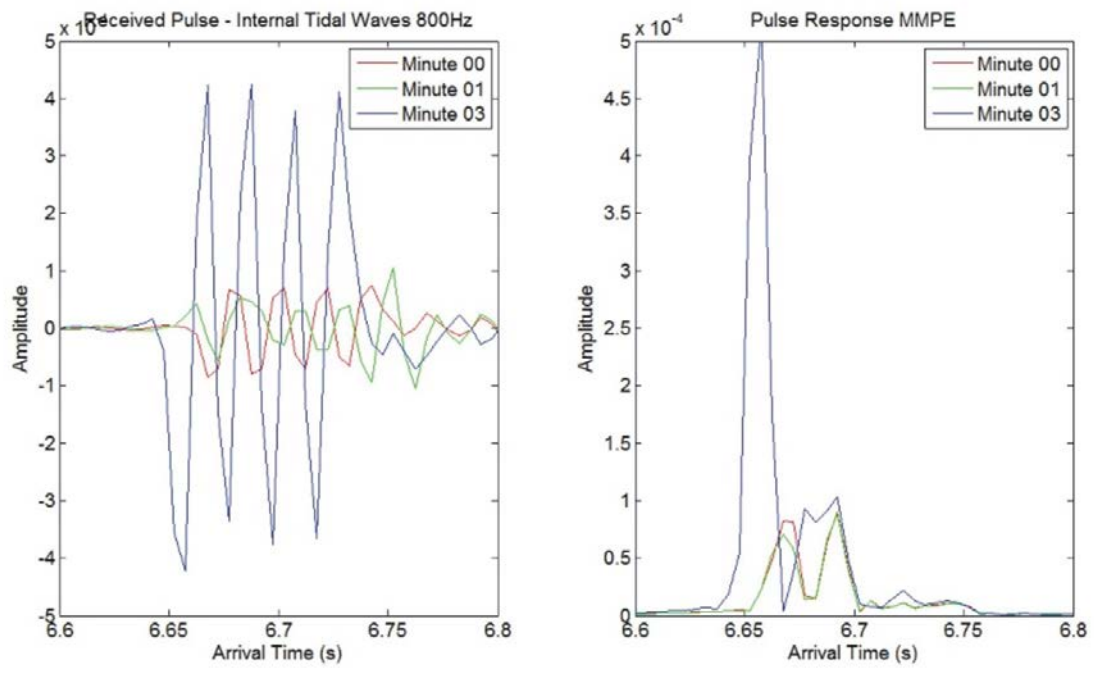


Figure 3.16: Received pulse and predicted Pulse Responses – IW SSP - 800Hz

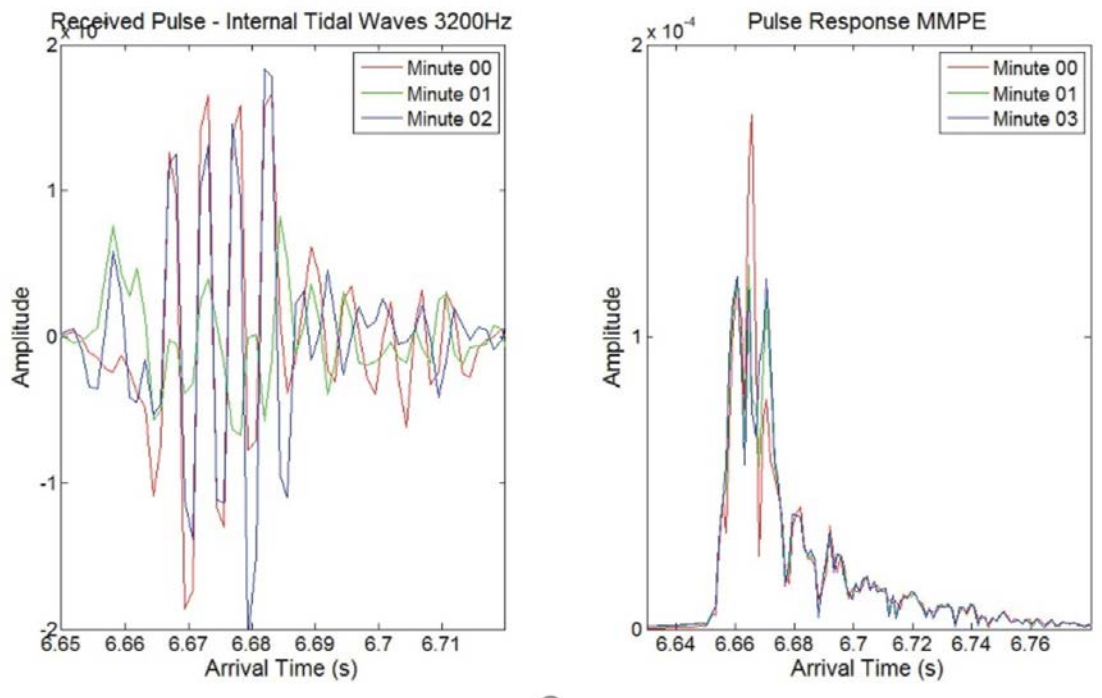


Figure 3.17: Received pulse and predicted Pulse Responses – IW SSP - 3200Hz

### Isothermal IW SSP – 800Hz

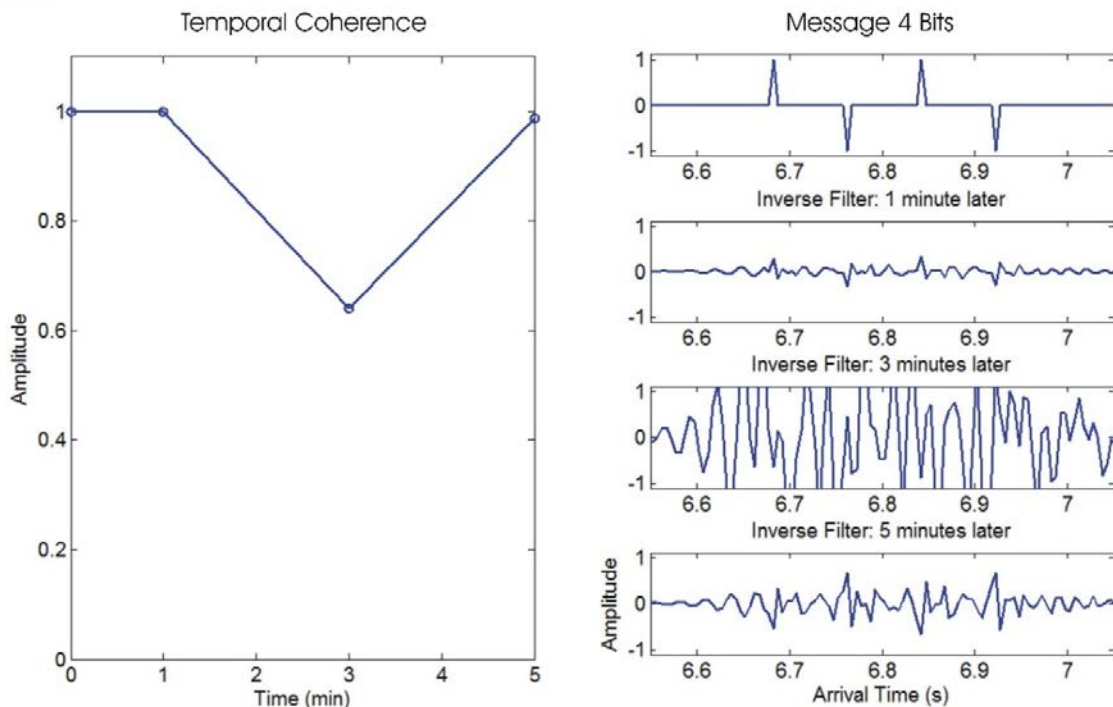


Figure 3.18: Temporal Coherence and Inverse Filter 800Hz - IW SSP

### Isothermal IW SSP – 3200Hz

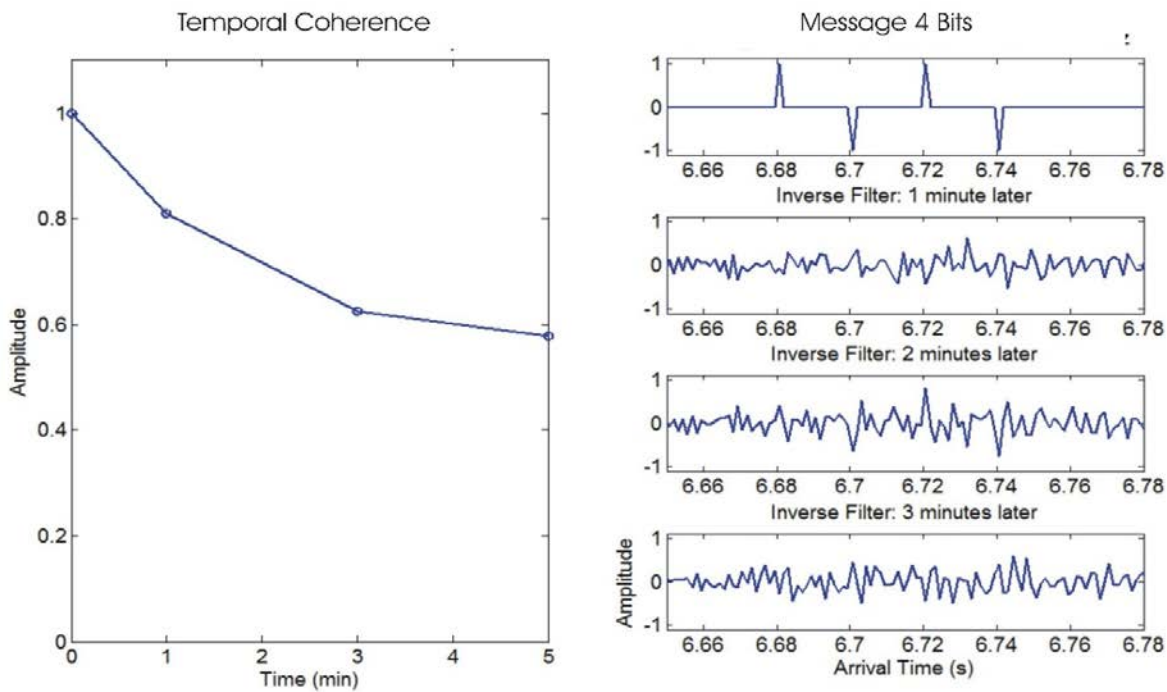


Figure 3.19: Temporal Coherence and Inverse Filter 3200Hz - IW SSP



### 3.2 – DISCUSSION

The results presented in this chapter were based, basically, on the sound speed profiles for each ocean temperature condition. The modeling did not consider any other causes for ocean fluctuations such as range dependence fluctuation in bathymetry and SSP and also bottom scattering, surface waves and so on. However, even being considered not realistic compared to a real ocean, the results for coherence and the inverse filter refresh times for each SSP are still useful to improve understanding over acoustic propagation in this shallow water channel in which upwelling occurs during the year. The results showed how difficult it is to keep up with rapidly changing ocean conditions. Based on these results, one can expect more difficulty to establish reliable communications just having previous knowledge about the ocean temperature and wind conditions.

Several previous research observations established that ocean remains coherent for about 2 minutes in most cases, enough to permit transmissions of M-Sequences. As an example, a 2047 bits M-Sequence is transmitted at 3200Hz in only 2.55 seconds and in approximately 10 seconds at 800Hz.

Next chapter, a new method to solve this phase decorrelation in time problem, measuring the pulse response and retrieving a message, simultaneously, using M-sequences is presented, thereby improving the performance of the communication system.

## CHAPTER 4

### **METHOD TO IMPROVE UNDERWATER DIGITAL COMMUNICATIONS USING M-SEQUENCES**

A unique method to optimize the underwater communications in shallow waters is presented in this chapter, being the main contribution of this thesis to ocean acoustics.

As the loss of coherence in the ocean is a serious issue, degrading severely the underwater communications, a method to retrieve a transmitted message through a shallow water channel, based only on predicted pulse responses from MMPE model and an inverse filter was presented in previous chapter. Based on those results, one could estimate the refresh time for the filter kernel to resolve the temporal variability of the channel for reliable communications. Conversely, the new method directly measures and updates the channel pulse response using M-Sequences and Fast Hadamard Transform properties, while collecting the transmitted message, simultaneously, taking advantage of the short M-sequences transmission times, during which the ocean can be still considered coherent. Therefore, a bit stream composed of a message embedded in a M-sequence transmitted through a noisy environment could be retrieved by a receiver, despite the severe multipath spreading and inter-symbol interference, with encouraging results in terms of BER.

The goals of this chapter are to present the new method and to discuss some results for real channel propagation conditions, emphasizing advantages for the establishment of reliable underwater communications in these shallow waters.

#### 4.1 – DESCRIBING THE METHOD

Briefly, a binary stream is created from a summation, sample by sample, of two other binary sequences of same length (2047 bits) but different intensities: a M-sequence (strong signal) and a Message (weak signal). The message, several times weaker, is spread along the M-sequence forming the Bit Stream. So, the bit stream M-Sequence+Message is convolved to a predicted channel pulse response from MMPE model and some additive white Gaussian noise is added, simulating a real transmission through the underwater channel.

At receiver, the simulated distorted bit stream, accounting for both inter-symbol interference and multipath spreading, is energy pulse compressed by the Fast Hadamard Transform, providing the measured channel pulse response, stored to be used in the matched filter ahead. Due to its perfect correlation, the compressed M-sequence high energy is located at the beginning of the stream being  $10 \cdot \log_{10}(P)$  decibels above the environmental noise. As the message is the desired information, being the M-sequence just a carrier, one can use the coordinate zeroing method (HCC0), developed by Chang, to eliminate the interference between the strong and the weak signals. At this point, the former bit stream is composed only by the message buried in noise which is inverse hadamard transformed, decompressing the low message energy. Last step, assuming perfect synchronization, the remaining sequence is correlated or matched filter to the previous measured channel pulse response, providing the desired message. The method performance is then analyzed in terms of bit error rate as follows:

$$\text{Bit Error Rate (BER)} = \frac{\text{\# Bits in Error}}{\text{\# Transmitted Bits}}$$

## 4.2 - SIMULATION PARAMETERS

The method will be presented and tested for two different amplitude relations for M-Sequence and Message: 10/1 on the left and 10/5 on the right of figure 4.1.

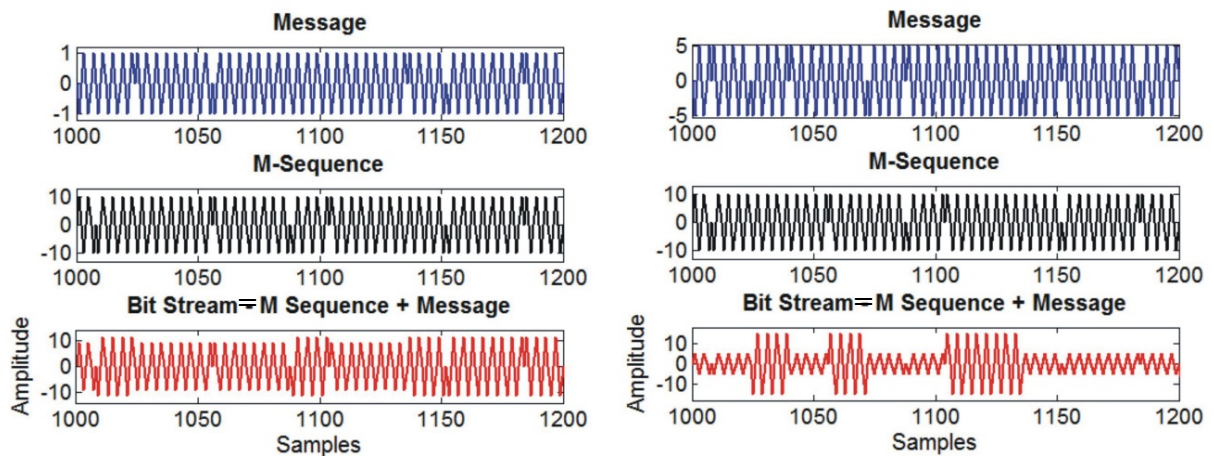


Figure 4.1: Bit streams composed of M-Seq + Message

In figure 4.1, one can verify that different intensity relations between the sequences affect the shape of the composed Bit Stream to be transmitted. Later, will be shown that retrieval of the message by the presented method and the performance of the communication system in terms of bit error rates in a noisy channel are directly related to the intensity of the message hidden in the M-sequence and the background noise level.

To simulate the channel propagation, the MMPE model predicted the pulse responses for several environmental conditions, as follows:

- Range: 10Km;
- Channel depth: 50 and 200m;
- Source/Receiver depths: 30m/15m and 120m/60m;
- Frequency of transmission: 3200Hz.

Furthermore, some additive white Gaussian noise over the Bit stream will make simulations more realistic, permitting comparisons and system performance analysis.

### 4.3 - RESULTS

#### **Case I: Channel depth: 50m**

Based on predicted pulse responses from chapter 3, for an upwelling event SSP (figure 3.2) and using a relation between M-sequence and Message of 10/1, a received Bit Stream composed of 2047 bits was simulated and transmitted in about 2.5 seconds at 3200Hz. In figure 4.2, one can verify the channel pulse response predicted by the MMPE model and the simulated bit stream transmitted through the channel, for a SNR of 10 dB over the M-sequence but just -10 dB over the buried message. One can observe that averaging of several M-sequences will not be performed to increase the SNR. Usually, averaging is performed during real ocean acoustic experiments to increase the SNR. However, only FHT compression will provide the gain in this work.

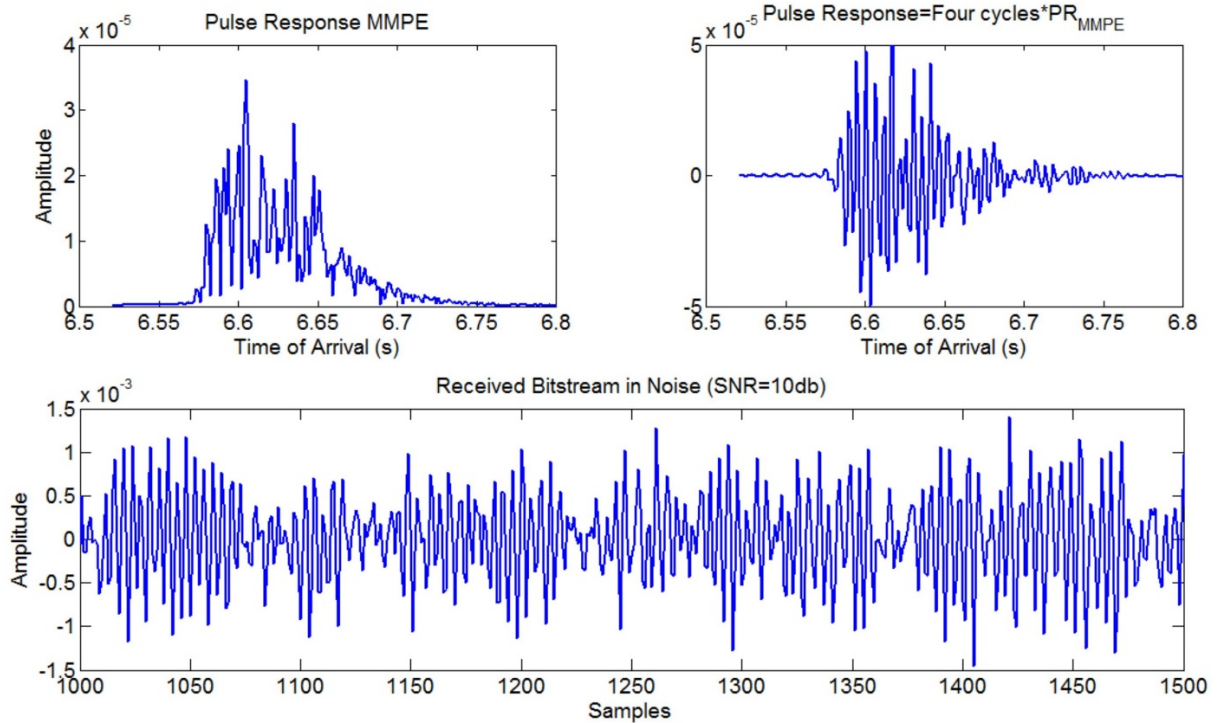


Figure 4.2: Predicted PR and received Bit Stream in noise – Channel depth 50m/3200Hz

Next, the received sequence, accounting for multipath and inter-symbol interference, is Hadamard transformed, providing the measured channel pulse response, exactly the same shape of that estimated by the MMPE model, as expected. Furthermore, due to the perfect correlation characteristic of the M-sequence, the pulse compressed to be coordinate zeroed is about 30 dB or  $10\log_{10}(2047)$  above the noise. This processing gain is shown in the left upper graph of figure 4.3.

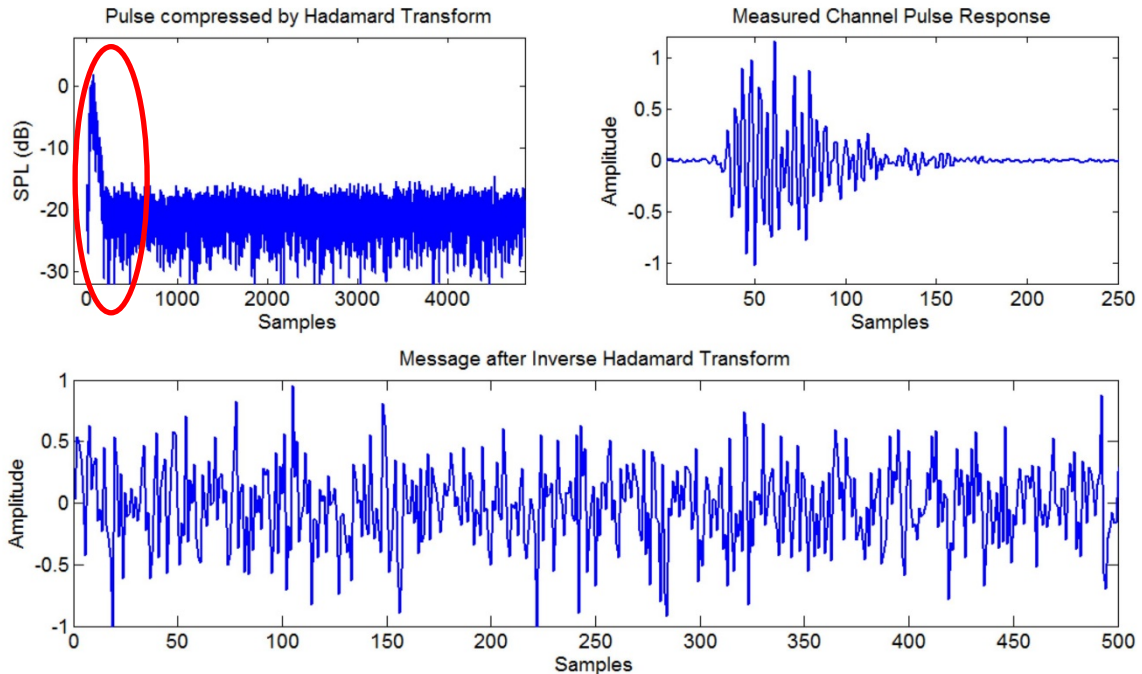


Figure 4.3: Above, processing gain (left), measured channel PR (right).  
Below, message after IFHT – Channel depth: 50m/3200Hz

Performing the inverse hadamard transform of the remaining sequence, a new sequence composed of the desired message buried in noise appears. Last step of the method, the new sequence is correlated or matched filtered to the measured channel pulse response, letting us to retrieve the originally transmitted message with some bit errors, being the performance stated in terms of Bit Error Rates in item 4.4. In figure 4.4, one can observe some samples of the originally transmitted message and the retrieved one, with the bit errors highlighted in red. These errors are common and are related to the SNR and amplitude relations between M-sequences and message. Typically, high SNR improves bit detection and low SNR affects the filter performance, causing bit errors. So, the number of bits in error are important and one must play with some transmission parameters (power, SNR...) in order to try to keep the BER as low as possible.

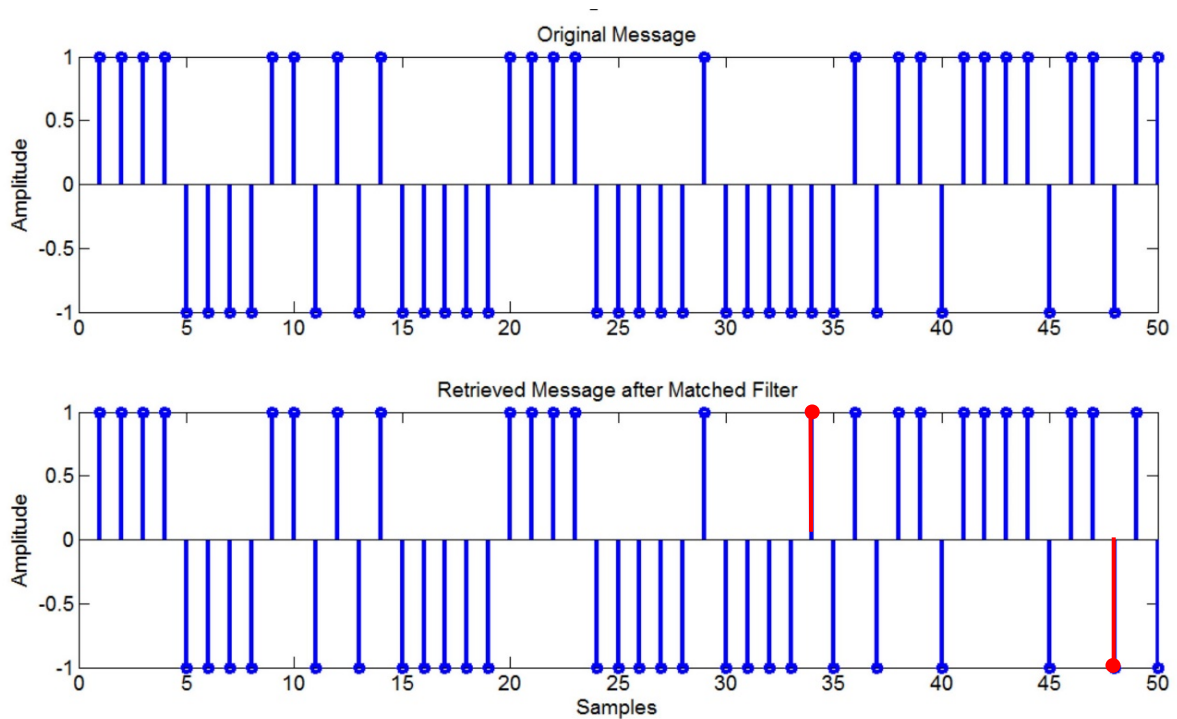


Figure 4.4: Transmitted/Retrieved message after matched filter - 50m/3200Hz  
Bit errors showed in Red

### Case II: Channel depth: 200m

The method's performance and validity was also verified for another channel depth: 200m, a typical depth near to the border of the continental shelf. For this simulation, the source was located at a depth of 120 meters, the receiver at 60 meters and the SSP, obtained by CTD casts in the study area showing a negative profile, was used. Furthermore, the temporal coherence time will be assumed to be approximately 2 minutes, the same of the 50m deep channel, considered in previous chapter.

By analyzing the predicted channel pulse response from the MMPE model, it is obvious that the acoustic field is deeply influenced by the sound reflections and refractions along the channel range, and by sound reverberation. Again, as done in case I, a relation between M-sequence and message of 10/1 was used to show the method



simulation. Therefore, one can check the MMPE channel pulse response and the simulated transmitted bit stream, for a SNR of 10dB over M-sequence, as shown in figure 4.5 below. For this case, due to the acoustic field reverberation, the predicted channel pulse response shape is different, presenting severe multipath and inter-symbol interference.

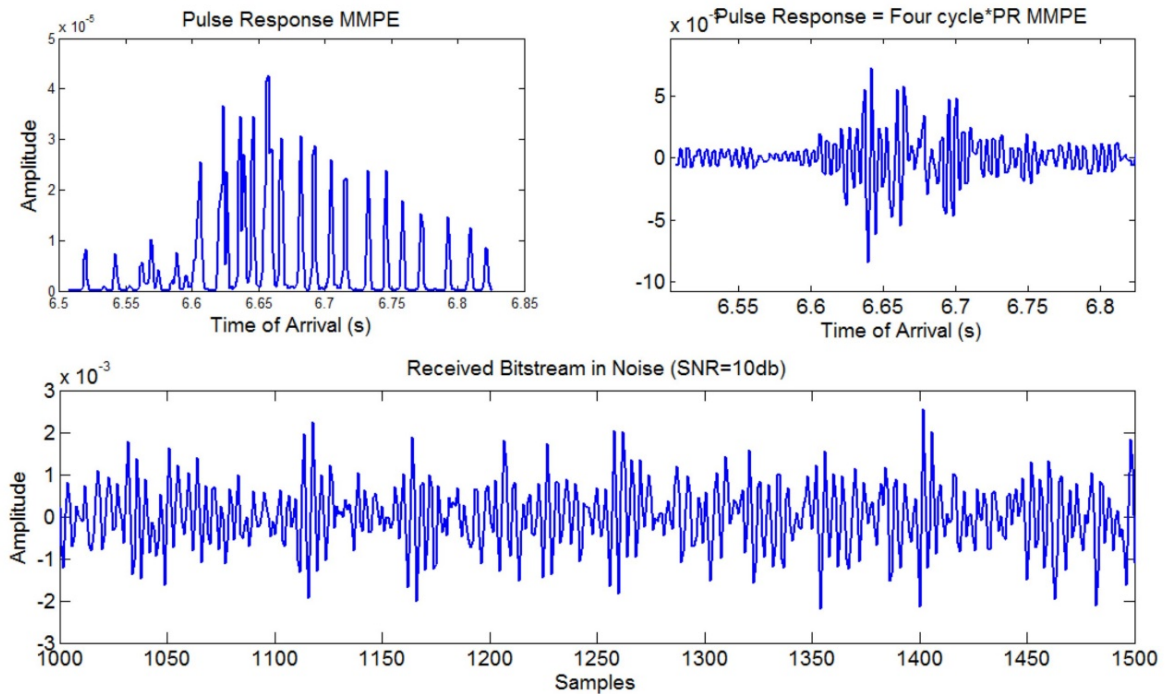


Figure 4.5: Predicted PR and received Bit Stream in noise for a 200m deep channel.

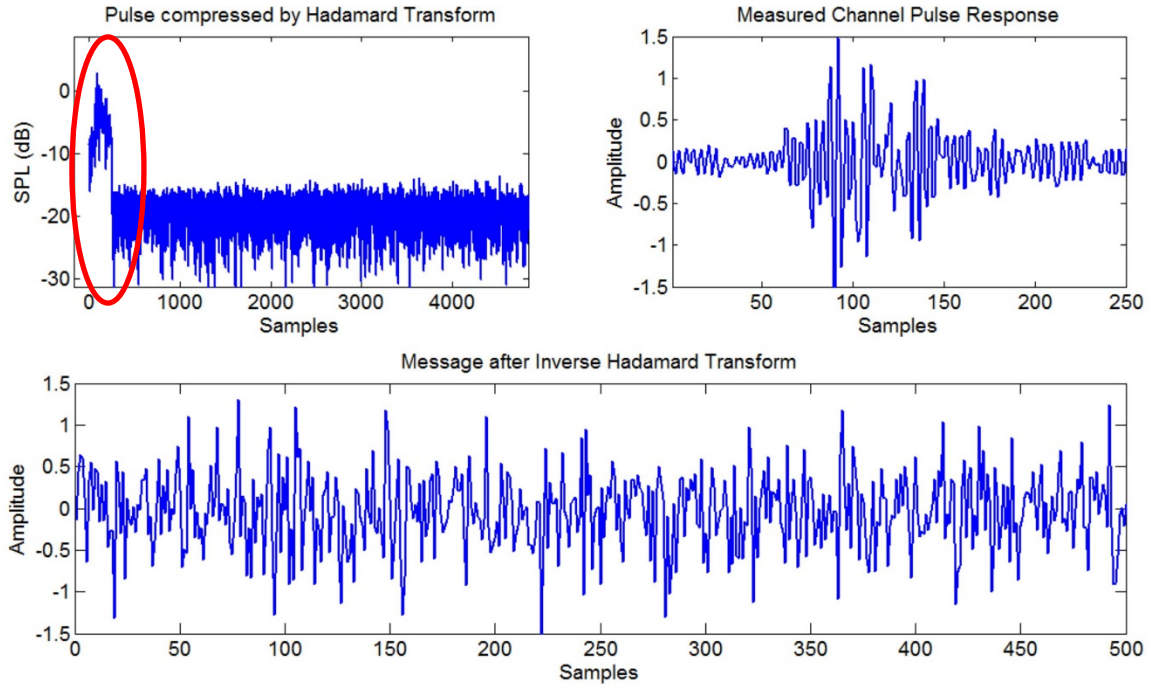


Figure 4.6: Above, processing gain (left), measured channel PR (right).  
Below, message after IFHT.

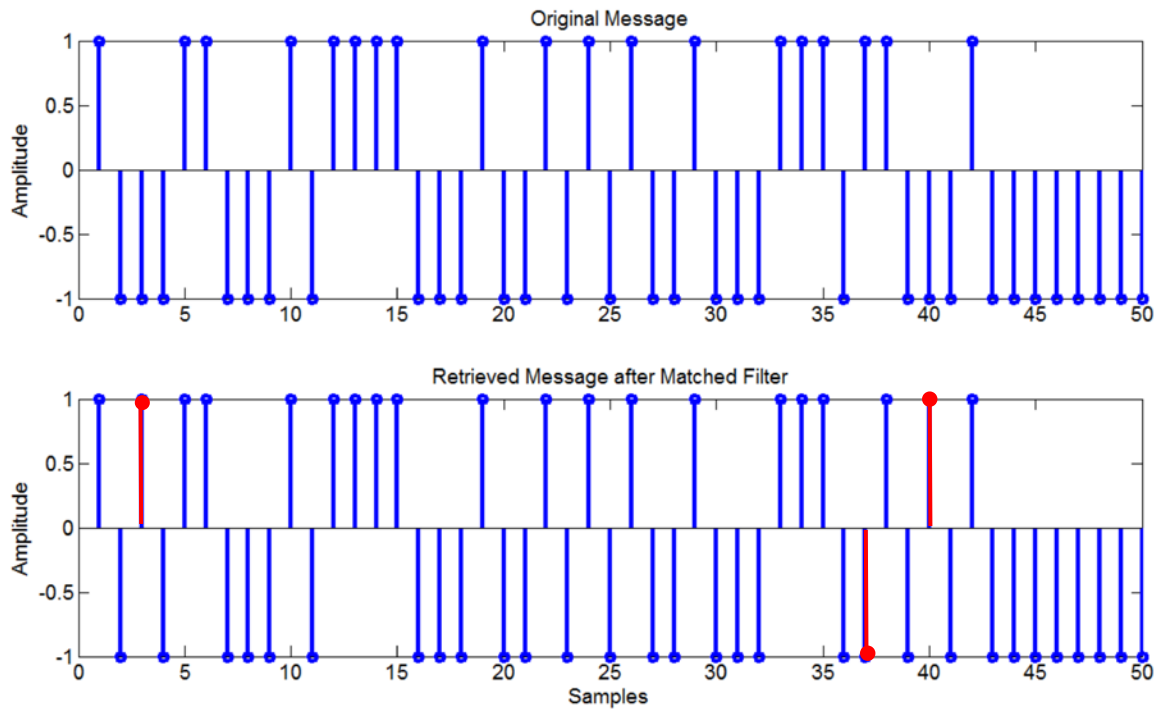


Figure 4.7: Transmitted/Retrieved message after matched filter - 200m/3200Hz  
Bit errors showed in Red

In the upper left of figure 4.6, the processing gain highlights the compressed pulse energy to be coordinate zeroed. The method presented good results for this deeper channel as well, compared to the other case. In figure 4.7, some bit errors in the retrieved message after the matched filter are highlighted in red. The occurrence of bit errors are absolutely normal being related to some parameters such as SNR and the amplitude relation between the M-sequence and the Message. However, to keep the system working accordingly, these errors must be kept as low as possible, avoiding loss of information.

The results, presented next, prove that the method is consistent for different channel configurations and several background noise levels, permitting retrieval of the transmitted message with good BER even in a low SNR channel condition.

#### **4.4 –NOISE LEVEL AND AMPLITUDE RELATIONS OVER BER**

The above analysis done for an amplitude relation of 10/1, could also be done for several other relations between the M-sequence and the Message to be transmitted. Each choice of the amplitudes influence directly over the message retrieved in the end of the method. Another parameter that affect the system performance is the channel background noise level. Therefore, to gain some knowledge over the influence of these parameters over the system, some simulations were done, for a range of SNR for the following amplitude relations: 10/1 and 10/5. The results, in terms of Bit Error Rates, are shown in both table 4.1 and figures 4.8 and 4.9.

Amplitude relation: 10/1					
SNR (dB)		Channel depth: 50m		Channel depth: 200m	
M-Sequence	Message	Bit Errors	BER	Bit Errors	BER
15	-5.02	18	0.9%	36	1.7%
10	-9.95	119	5%	134	6.5%
5	-15.06	336	15%	337	16%
2	-18.01	521	25%	489	24%

Table 4.1: Amplitude 10/1, SNR and BER for 50m and 200m deep channel

Amplitude relation: 10/5					
SNR (dB)		Channel depth: 50m		Channel depth: 200m	
M-Sequence	Message	Bit Errors	BER	Bit Errors	BER
15	8.05	0	0%	1	0.048%
10	2.98	2	0.1%	4	0.2%
5	-1.88	4	0.2%	10	0.5%
2	-4.98	10	0.5%	22	1%
0	-7.07	42	2%	46	2.2%

Table 4.2: Amplitude 10/5, SNR and BER for 50m and 200m deep channel

From the above table, one can compare the different signal to noise ratios over the M-sequence and the Message, related to their amplitudes. Comparing the BER for a bit stream relation of 10/1 to 10/5, for the same SNR (table 4.1), one can check that the system performance is much better for 10/5 than 10/1 amplitude relation. Thus, increasing the amplitude of the hidden message, the SNR is also increased, providing better results in terms of BER.

An important conclusion here is that the method's message retrieval is efficient both in high or low SNR. Focusing on low SNR, a more interesting and challenging situation, from table 4.1, one can verify that even for a SNR of approximately -5 dB over the hidden message, for a 10/5 relation, the BER is around just 1% which can be considered reasonable for a rapidly time variant propagation channel. Thus, depending on the estimated noise level of the channel, one could play with the sequences amplitude relation in order to improve system performance or just average some sequences to increase the SNR, retrieving messages with low BER.

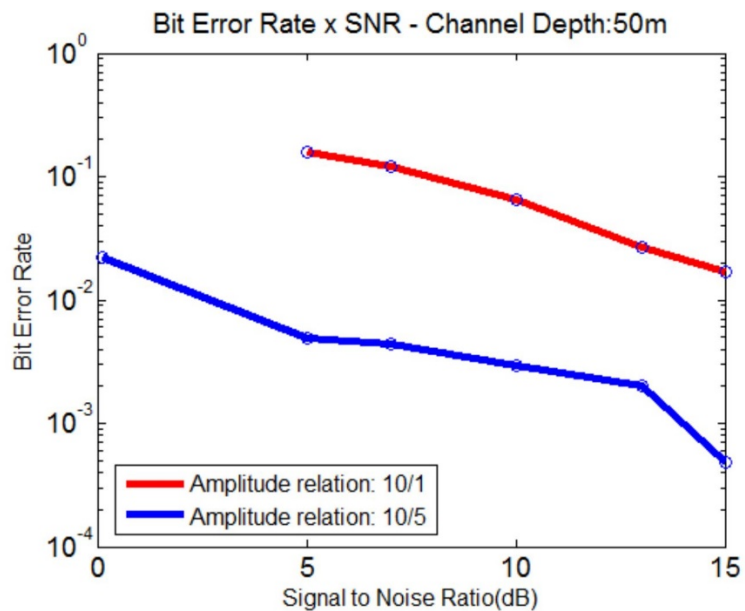


Figure 4.8: Estimation of BER for several SNR for a 50m deep channel

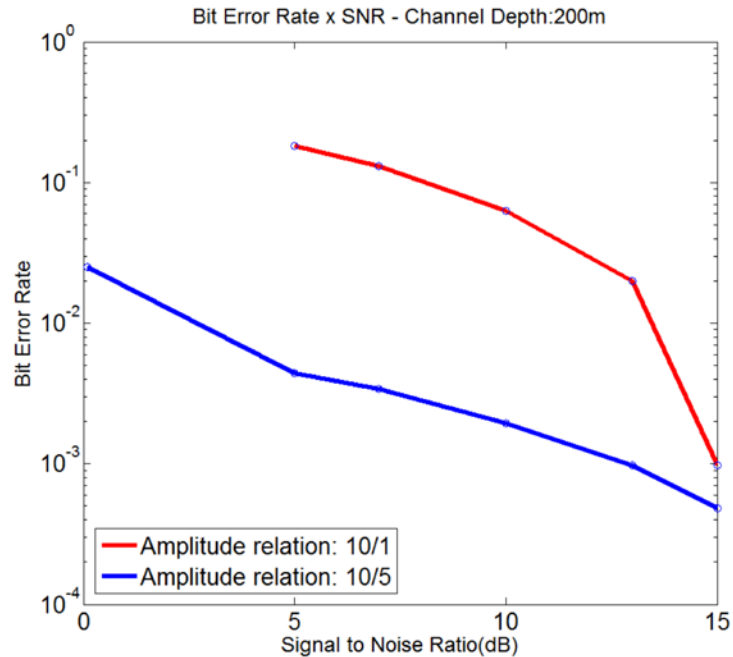


Figure 4.9: Estimation of BER for several SNR for a 200m deep channel

#### 4.5 – DISCUSSION

The simulations above showed that this unique method appears efficient in retrieving the transmitted message through the channel, presenting several advantages, even for low SNR, around 0 dB. First, as shown in figure 4.1, bit streams for amplitude relations of 10/1 and 10/5, even looking very different, look like just noise for someone intercepting the communications because M-sequences are known as pseudo-random noise sequences and can be modified at each transmission, making harder the message identification. Furthermore, the M-sequence tracks the channel modifications in time, providing the desired channel pulse responses essential to correlation or matched filter in the end of the method. Also, the processing gain of about 30 dB after the M-sequence Hadamard transform let one to correctly estimates or measures the channel pulse response, vital to the good performance of any communication system.

As mentioned in chapter 3, the temporal coherence of the channel plays a key role in underwater acoustic communications. In the same chapter, the 50m deep channel showed coherence times around 2 minutes, for a SSP from an upwelling event, and assumed here the same temporal coherence for a 200m deep channel. However, for a transmission frequency of 3200 Hz, the 2047 bits M-sequence of the presented method takes about only 2.5 seconds to be transmitted, much less than the channel coherence time and so, solving the complicated phase decorrelation problem that arises when phase coherence is lost. It means that the channel is coherent during the transmission time, permitting the use of the measured channel pulse response to keep up with the multipath and inter-symbol interference, correlating and retrieving the message accordingly.

In this work simulations, no averaging or M-Sequence stacking were done, as usual at sea, being all processing gain due to the pulse compression by the FHT and matched filter only. Thus, in a future experiment, the summation between the presented method with some averaging could improve the SNR, permitting the retrieval of the transmitted message with even better BER.

Concluding, the method presented here is promising and can be a useful tool to improve underwater acoustic communications in both civilian and military applications, even that the thesis results are based only on modeling and computer simulations. Thus, the Brazilian Navy could perform some field experiments not only between fixed stations but also between ships and submarines in the future to deal with Doppler effects, another complicating factor related to moving platforms, and this way, take full advantage of this new method in advance.

## CHAPTER 5

### CONCLUSIONS AND FUTURE WORK

In this thesis an underwater acoustic communication system was simulated to study the channel temporal coherence under some propagation conditions, and to present a new method to retrieve the transmitted message using M-sequences.

First, it has been shown based on simulations that the temporal coherence is directly related to the inverse filter kernel refresh times. In a real world, the channel SSP are both depth and range dependent. Nevertheless, the simulations were based on only one SSP for the whole channel range and even thus several conclusions could be extracted.

For each SSP gradient: isothermal warm/cold, upwelling and internal waves, the acoustic field presented different multipath and inter-symbol-interference due to interactions between the sound waves and the boundaries. The channel coherence times varied significantly for all these cases. For almost isothermal SSP (warm/cold), the inverse filter retrieved the message correctly for a time longer than 5 minutes, before the inverse filter kernel update based in a fresh predicted channel pulse response. In some cases, it was observed that phase turned around from zero to 180 and to zero again, in a time frame of several minutes. This phase decorrelation looked much more like a deterministic than a random phenomenon. But the acoustic field was very different for negative gradient SSP such as during upwelling events and internal waves passages. For these cases, the coherence was lost after about 1 to 2 minutes due to random phenomena, much faster than the previous cases.

Thus, for a fixed or land station which relies only on predicted channel pulse responses from an acoustic model to update the kernel of the inverse filter, it is important



to be able to measure the SSP periodically, according to the estimated coherence times, in order to let the system retrieve the message with reasonable performance.

Next, a new method to optimize the underwater communications in shallow waters, using M-sequences, was presented. The ocean environment is fast varying, changing rapidly its characteristics, which affects directly any underwater acoustic propagation. So, it is vital to any communication system to measure or estimate correctly the channel pulse response to undo the inter-symbol interference caused by the multipath and so collect the message accordingly.

The method transmitted a bit stream composed of a strong and a weak signal, continuously measuring and updating the channel pulse response while sending a message, simultaneously. Also, it was based on some important concepts such as the perfect correlation of M-sequences, Hadamard transforms and coordinate zeroing of pulse energy (Chang, 1992). The processing gain after the Hadamard transform, around 30 dB over noise, using a 2047 bits M-sequence, permitted the coordinate zeroing and so the elimination of the interference between the M-sequence and the message.

The results, in terms of Bit Error Rates, for the simulated propagation in a noisy channel were very encouraging. The observed BER for both amplitude relations were good but the method provided better results when the message amplitude were increased, from 10/1 to 10/5. For both cases, even for low SNR, around 2 dB, the method improved the BER and thus, the retrieved message as desired. Therefore, depending on the goal of the experiment, the researcher can play with some parameters, such as M-Sequence and message amplitudes, in the real ocean to improve results.

The method is promising but must be tested at sea for fixed sources and receivers. The plan is to extend the method for moving sources such as ships and submarines, a more interesting and useful case for the Brazilian Navy. Several and challenging additional problems are expected at this point. Faster loss of coherence and Doppler effects will probably play a role in these new propagation conditions complicating the retrieval of the transmitted messages. But a method to deal with these Doppler effects were already previously described by DeFerrari and Rogers (2009) for another application, a starting point to help us to solve these news problems expected in underwater communications between moving vessels in shallow waters.

## REFERENCES

- Bjor, O. H. “Maximum length sequence”. Norsonic AS (2000).
- Lempel, A., Cohn M. “On fast M-sequence transform”, IEEE Trans. Inf. Theory (1977): 135 – 137.
- Chang H. S. “Detection of weak, broadband signals under Doppler-scaled, multipath propagation”. PhD Diss. Electrical Engineering Systems, University of Michigan, 1992.
- DeFerrari, H. A., A. Rogers. “Reducing active sonar source levels by continuous transmit and receive operation”. Journal of Underwater Acoustics 59 (2009): 5-18.
- DeFerrari, H. A., J. F. Lynch and A. Newhall. “Temporal coherence of mode arrivals”. Journal of the Acoustical Society of America 124, no.3 (2008): 104–109.
- DeFerrari, H. A., Wylie J., “Ideal signals and processing for continuous active sonar”, Journal of the Acoustical Society of America, Proceedings of Meetings on Acoustics 19 (2013).
- Etter, P. C. *Underwater acoustic modeling and simulation*. 3rd ed. New York: CRC Press, 2013.
- Jensen, F., W. Kuperman, M. B. Porter and H. Schmidt. *Computational ocean acoustics*. 2nd ed. New York: Springer, 2011.
- Jeruchim, M. C., B. Philip , K. S. Shanmugan. *Simulations of communication systems*. 2nd ed. New York: Kluwe Academic Press, 2002.
- Lourenco, F.M. “Temporal fluctuations of the sound speed field and how they affect acoustic mode structures and coherence”. MSc Thesis. Applied Marine Physics, University of Miami, 2012.
- Mackenzie, K.V., “Nine-term equation for sound speed in the oceans”. Journal of the Acoustical Society of America 70 (1981): 807–812.
- Massel, S. R. *Internal gravity waves in the shallow seas*. 1st ed. Switzerland: Springer International Publishing, 2015.
- Metzger, K., “Signal processing equipment and techniques for use in measuring ocean acoustic multipath structures”. Ph. D diss., University of Michigan, 1983.
- Proakis, J. G., S. Masoud. *Digital communications*, 5th ed. New York: McGraw-Hill Companies, 2008.

Rodrigues, R. F. “Upwelling at Cabo Frio (Brazil)”. MSc Thesis. Oceanography. Naval Postgraduate School, 1973.

Simões, M. V, F. Xavier, L. Barreira, L. Artusi, H. Macedo, Y. Alvarez and R. Romano. “Medições geoacústicas em sedimentos marinhos da plataforma continental próxima a Arraial do Cabo – Brasil”, 2ª Jornada de Engenharia Hidrográfica (2012), Lisbon-Portugal.

Smith, K. B., “Convergence, stability, and variability of shallow water acoustic predictions using a split-step Fourier parabolic equation model”, *Journal of Computational Acoustics* 9 (2000): 243-285.

Song, A., M. Badiey. “Channel simulation for underwater acoustic communication network”, *IEEE Journal of Oceanic Engineering* 35 (2010): 756–765.

Stienberg, J.C., T. G. Birdsall, “Fixed system acoustic propagation measurements in the Florida Straits”, *Journal of the Acoustical Society of America* 39 (1966): 301–315.

Stojanovic, M., J.A. Catipovic and J. G. Proakis. “Phase-coherent digital communications for underwater acoustic channels”. *IEEE Journal of Oceanic Engineering* 19 (1994): 100-111.

Stojanovic, M. “Underwater acoustic communication”. *Wiley Encyclopedia of Electrical and Electronics Engineering* (2003).

Stojanovic, M. “On the relationship between capacity and distance in an underwater acoustic communication channel”. *Proceedings of the First ACM International Workshop on Underwater Networks* (2006).

Torres Jr., A. R. “Resposta da ressurgência costeira de Cabo Frio a forçantes locais”. MSc Thesis. Sciences in Oceanic Engineering, Federal University of Rio de Janeiro, 1995.

Urick, R. J. *Principles of Underwater Sound*. 3rd ed., Peninsula Publishing, 1983.

Wylie, J. “The effects of random bottom bathymetry on coherence in shallow water acoustic propagation”. Ph.D diss., Applied Marine Physics, University of Miami, 2013.

Yang, T. C. “Measurements of temporal coherence of sound transmissions through shallow water,” *Journal of the Acoustical Society of America* 120, no. 5 (2006): 2595–2614.